

~~CONFIDENTIAL~~Copy 6
RM L50J06

NACA RM L50J06

~~NACA~~**RESEARCH MEMORANDUM**

INVESTIGATION OF A 42.7° SWEEPBACK WING MODEL TO
 DETERMINE THE EFFECTS OF TRAILING-EDGE THICKNESS
 ON THE AILERON HINGE-MOMENT AND FLUTTER
 CHARACTERISTICS AT TRANSONIC SPEEDS

By Robert F. Thompson

Langley Aeronautical Laboratory
 Langley Air Force Base, Va.

CLASSIFICATION CANCELLEDAuthority NACA R 7-2577 Date 8/31/54By mta 9/14/54 See _____
CLASSIFIED DOCUMENT

This document contains classified information affecting the National Defense of the United States within the meaning of the Espionage Act, USC 5031 and 32. Its transmission or the revelation of its contents in any manner to an unauthorized person is prohibited by law.
 Information so classified may be imparted only to persons in the military and naval services of the United States, appropriate civilian officers and employees of the Federal Government who have a legitimate interest therein, and to United States citizens of known loyalty and discretion who of necessity must be informed thereof.

**NATIONAL ADVISORY COMMITTEE
 FOR AERONAUTICS**

WASHINGTON
 December 26, 1950

UNCLASSIFIED

~~CONFIDENTIAL~~



3 1176 01436 2447

UNCLASSIFIED

1
NAGA RM L50J06

NATIONAL ADVISORY COMMITTEE FOR AERONAUTICS

RESEARCH MEMORANDUM

INVESTIGATION OF A 42.7° SWEPTBACK WING MODEL TO
DETERMINE THE EFFECTS OF TRAILING-EDGE THICKNESS
ON THE AILERON HINGE-MOMENT AND FLUTTER
CHARACTERISTICS AT TRANSONIC SPEEDS

By Robert F. Thompson

SUMMARY

An investigation was made in the Langley high-speed 7- by 10-foot tunnel of a 42.7° sweptback wing model to determine the effects of aileron trailing-edge thickness on aileron hinge moments and one-degree-of-freedom aileron flutter. The wing had an aspect ratio of 4.0, a taper ratio of 0.5, and was tested over a Mach number range of 0.60 to 1.175. The half-span, 20-percent-chord ailerons were flat sided and located outboard.

Increasing the trailing-edge thickness shifted the hinge-moment parameters $C_{h\delta}$ and $C_{h\alpha}$ in a negative direction and eliminated the reversal in $C_{h\delta}$ at supercritical speeds. The aileron having a trailing-edge thickness of one half the hinge-line thickness exhibited the least tendency to flutter, and flutter of the aileron with trailing-edge thickness equal to the hinge-line thickness occurred over a larger speed range.

INTRODUCTION

It is a fairly common experience with airplanes flown at high subsonic speeds, or when new designs are tested in high-speed tunnels, to find that a Mach number is reached where severe changes in aileron characteristics appear. These changes may appear as flutter, severe changes in hinge-moment characteristics, or even reversal of aileron effectiveness.

~~CONFIDENTIAL~~

UNCLASSIFIED

In an investigation of the lateral-control characteristics at transonic and supersonic speeds of a wing having a circular-arc airfoil section and 42.7° of sweepback of the leading edge (references 1 and 2), it was found that the original circular-arc contour aileron gave very low effectiveness in the transonic-speed range and that the effectiveness reversed for some conditions. While studying various ailerons to alleviate this condition, it was found that ailerons having flat sides and a thickened trailing edge improved the effectiveness and eliminated the reversal (references 1, 3, and 4).

The purpose of the present investigation of the 42.7° sweptback semispan wing model was to determine the effects of blunt trailing edges on aileron hinge moments and aileron flutter. Hinge moments were measured for three different ratios of trailing-edge to hinge-line thickness for a range of deflections and angles of attack through a Mach number range from 0.60 to 1.10. The flutter investigated is the tendency of the aileron to maintain steady or divergent oscillation about its hinge axis with only one degree of mechanical freedom and is referred to herein as "aileron buzz." To investigate this aileron buzz, the free-floating characteristics of the three ailerons were recorded through a Mach number range from 0.60 to 1.175. The effects of increasing moment of inertia were investigated on the aileron having a trailing-edge to hinge-line thickness ratio of 1.0. A comparison is given of the experimental flutter frequencies with the results computed by the empirical analysis of references 5 and 6. Aileron effectiveness parameter $C_{l\delta}$ and other aerodynamic characteristics can be found for the wing-aileron combinations in reference 3.

COEFFICIENTS AND SYMBOLS

C_h	aileron hinge-moment coefficient ($H/q2M'$)
H	aileron hinge moment measured about hinge line, foot-pounds
q	average dynamic pressure over span of model, pounds per square foot $\left(\frac{1}{2}\rho V^2\right)$
M'	area moment of aileron aft of hinge line about hinge line, cubic feet
b	twice span of semispan model (1 ft)
c	local wing chord, feet

c_a	aileron chord aft of hinge line, feet
y	spanwise distance from plane of symmetry, feet
ρ	mass density of air, slugs per cubic foot
V	average air velocity over span of model, feet per second
M	effective Mach number over span of model $\left(\frac{2}{S} \int_0^{b/2} cM_a dy \right)$
M_a	average chordwise local Mach number
M_l	local Mach number
S	twice wing area of semispan model (0.25 sq ft)
M_{cr}	Mach number at which sonic velocity is first attained on section of wing at zero lift
α	angle of attack of wing relative to air stream, degrees
δ	aileron deflection measured perpendicular to hinge line, degrees
t	ratio of aileron thickness at trailing edge to thickness at hinge line
R	Reynolds number based on mean aerodynamic chord (0.259 ft)
θ	included angle of aileron trailing edge, measured parallel to air stream, degrees

$$C_{h\delta} = (\partial C_h / \partial \delta)_{\alpha}$$

$$C_{h\alpha} = (\partial C_h / \partial \alpha)_{\delta}$$

The subscripts outside the parentheses indicate the factors held constant during the measurement of the parameters in the vicinity of $\delta = 0^\circ$ and $\alpha = 0^\circ$, respectively.

MODEL AND APPARATUS.

The wing of the semispan, wing-fuselage model used for this investigation had a leading-edge sweepback of 42.7° , a taper ratio of 0.50, an aspect ratio of 4.0 and was made of steel with a polished surface. A drawing of the model is given as figure 1. The wing had a 10-percent-thick circular-arc airfoil section normal to the 50-percent-chord line and was approximately 8 percent thick parallel to the air stream. The semispan wing was mounted as a midwing with no dihedral or incidence in a polished-brass fuselage that was semicircular in cross section and curved to conform to the bump contour (fig. 1). The wing-fuselage combination was bolted rigidly to the bump surface at the desired angle of attack.

The 20-percent-chord, 50-percent-span, outboard ailerons were hinged to the wing with a hinge pin at the wing tip and a hinge rod passing through the wing along the 80-percent-chord line to the chamber within the bump. Hinge moments were measured by a calibrated beam-type strain gage clamped to the hinge rod within the bump. The interchangeable ailerons were unsealed and had ratios of trailing-edge to hinge-line thickness of $t = 0$, $t = 0.5$, and $t = 1.0$.

The ailerons were constructed by gluing spruce to a duralumin spar and were mass balanced about the hinge line by a lead overhang nose balance. The elliptical nose was the same for all ailerons, and the overhang was approximately 30 percent of the aileron chord aft of the hinge line. The aileron system was mass balanced to prevent any coupled wing-aileron flutter. Balance weight was spaced along the span to minimize any twisting moment due to variable mass. The moment of inertia I of each aileron system is given in table I. The moment of inertia of the aileron with a thickness ratio of 1.0 was increased by attaching various brass disks to the hinge rod within the bump surface.

Free-floating characteristics of the ailerons were measured by replacing the strain gage with a reluctance-type pickup instrument consisting of a small vane attached to the hinge rod which varied the air gap between two coils. Readings of this pickup were recorded against time by an oscillograph. The reading element of the oscillograph would measure frequencies to about 500 cycles per second. Amplitude of aileron motion was determined from a static calibration and no attempt was made to determine dynamic effects on this calibration. The aileron motion was unrestrained. No friction measurements were made since they were believed to be small and approximately the same for each aileron.

The ailerons had a small amount of freedom in translation due to the plain type of bearings used. This movement was kept to a minimum and checked after each run. After one set of runs, it was found that

the hinge play had increased due to wear. The bearings were reworked to decrease the freedom, and check runs showed no appreciable change in the frequency or amplitude of aileron motion.

TESTS AND CORRECTIONS

The tests were made in the Langley high-speed 7- by 10-foot tunnel and utilized an adaptation of the NACA wing-flow technique for obtaining transonic speeds. The technique used involves the mounting of a model in the high-velocity flow field generated over the curved surface of a bump located on the tunnel floor (see reference 7).

Typical contours of local Mach number in the vicinity of the model location on the bump, obtained from surveys with no model in position, are shown in figure 2. It is seen that there is a variation of Mach number of about 0.07 over the model semispan at the lower Mach numbers and of about 0.10 at the high Mach numbers. The chordwise variation is generally less than 0.01. The effective Mach number over the wing semispan is estimated to be 0.02 higher than the effective Mach number where the 50-percent-span outboard ailerons are located. No attempt has been made to evaluate the effect of this chordwise and spanwise Mach number variation. The long-dashed line shown near the root of the wing in figure 2 indicates a local Mach number that is 5 percent below the maximum value and represents the extent of the bump boundary layer. The effective test Mach number was obtained from contour charts similar to those in figure 2 by use of the relationship

$$M = \frac{2}{5} \int_0^{b/2} cM_a dy$$

The variation of Reynolds number with Mach number for average test conditions is presented in figure 3. Reynolds number is based on the wing mean aerodynamic chord (0.259 ft).

Hinge moments were obtained for three aileron trailing-edge-thickness ratios (fig. 1) through a Mach number range of 0.60 to 1.10, an angle-of-attack range of 0° to 5°, and at various aileron deflections. The aileron deflection was determined from the initial setting and the amount the hinge rod deflected under load. This deflection was very large at the high aileron angles and Mach numbers (about 50 percent of the initial aileron deflection at the extreme test conditions).

Free-floating characteristics of the three ailerons were recorded through a Mach number range from 0.60 to 1.175 at $\alpha = 0^\circ$. Preliminary tests were made with the wing tip braced as shown in figure 4. The tip brace eliminated wing bending and torsion as nearly as possible and allowed the aileron only one degree of mechanical freedom. Removing the tip brace had no appreciable effect on aileron motion, and all tests reported herein are with the tip unrestrained, as shown in figure 5.

RESULTS AND DISCUSSION

Hinge-Moment Characteristics

The rate of change of hinge-moment coefficient with aileron deflection increases negatively with increasing δ for the aileron with $t = 0$ except for a range of δ of $\pm 4^\circ$ at $M = 0.95$ and $M = 1.00$ (fig. 6) and decreases negatively with increasing δ for the ailerons with $t = 0.5$ and $t = 1.0$ (figs. 7 and 8). Additional test data were obtained for the aileron with $t = 1.0$, as shown on figure 8, to determine whether or not the hinge moment reversed over a small range of δ in the vicinity of $\delta = 0^\circ$ after flutter was found at subcritical speeds for this aileron. The ailerons do not trim at $\delta = 0^\circ$ due to asymmetry of aileron construction.

The rate of change of hinge-moment coefficient with angle of attack decreases positively with increasing α throughout the speed range for the aileron with $t = 0$ (fig. 9) and decreases negatively with increasing α up to $M = 0.85$ for the ailerons with $t = 0.5$ and $t = 1.0$ (figs. 10 and 11). Above $M = 0.85$, the variation with α for the ailerons with $t = 0.5$ and $t = 1.0$ is linear except for the aileron with $t = 0.5$ from $M = 0.90$ to $M = 1.0$ where C_h decreases positively with increasing α . No test-data points were plotted on figures 9, 10, and 11 since, owing to the load deflection correction, it was necessary to cross plot the test data to obtain values of C_h at $\delta = 0^\circ$.

The variation of the hinge-moment parameter $C_{h\delta}$ (measured at $\delta = 0^\circ$) with Mach number is given in figure 12. The values of $C_{h\delta}$ for the conventional, straight-sided aileron ($t = 0$) do not vary with Mach number up to $M = 0.87$ and, for the configuration tested, $C_{h\delta}$ is underbalanced. Above $M = 0.87$, which is the critical Mach number of the wing, abrupt and large variations in $C_{h\delta}$ occur with increasing Mach number and the aileron becomes overbalanced in the speed range from $M = 0.92$ to $M = 1.02$. The large positive (overbalanced) values

of $C_{h\delta}$ in the reversal range did not extend over the entire aileron-deflection range but did cover a large portion of the useful operating range, as shown at $M = 0.95$ and $M = 1.00$ in figure 6. The rapid changes, reversal, and heaviness of hinge moments for the aileron with $t = 0$ result in unsatisfactory hinge-moment characteristics at supercritical Mach numbers for the speed range tested. This is the same Mach number range where reversal and loss of aileron effectiveness occurred for the aileron with $t = 0$ (references 1 and 2).

Increasing the trailing-edge thickness to one half the hinge-line thickness (aileron with $t = 0.5$) results in a large shift in $C_{h\delta}$ in a negative direction and eliminates any reversal tendency at supercritical speeds. The values of $C_{h\delta}$ have a relatively small negative increase with Mach numbers from $M = 0.6$ to $M = 0.95$. Above $M = 0.95$, there is an abrupt increase in control heaviness until supersonic Mach numbers are reached. This variation would result in a general increase in underbalanced control forces with aileron deflection throughout the speed range, especially above $M = 0.95$, but the undesirable effects of hinge-moment reversal would not be encountered.

Increasing the trailing-edge thickness until it was equal to the thickness at the hinge line (aileron with $t = 1.0$) resulted in a further negative shift in $C_{h\delta}$, with the same general variation of $C_{h\delta}$ with Mach number as the aileron with $t = 0.5$. The rapid negative increase in $C_{h\delta}$ for the aileron with $t = 1.0$ occurred at a lower speed and was not as abrupt as with the aileron with $t = 0.5$.

The effects of Mach number on the hinge-moment parameter $C_{h\alpha}$ are given in figure 13. The values of $C_{h\alpha}$ for the aileron with $t = 0$ were positive throughout the speed range tested and did not vary up to the critical speed of the wing. Above this speed rapid changes occurred. Increasing the trailing-edge thickness shifted $C_{h\alpha}$ in a negative direction. The magnitude of the shift was generally larger for the increase of t from 0 to 0.5 than for the increase of t from 0.5 to 1.0. The values of $C_{h\alpha}$ had the same general variation with Mach number for the three trailing-edge-thickness ratios tested, although the changes in $C_{h\alpha}$ with Mach number occur at slightly lower speeds for the ailerons with $t = 0.5$ and $t = 1.0$.

This negative shift in $C_{h\delta}$ and $C_{h\alpha}$ with increasing t agrees with results obtained at $M = 0.055$ (reference 8) and at $M = 1.9$ (reference 9). Increasing the trailing-edge thickness produced effectively the same results on hinge moments as decreasing the

trailing-edge angle (reference 10). The included angle of the trailing edge θ , indicated on figure 1, is measured in a plane parallel to the air stream. The critical trailing-edge angle, as recommended in reference 10, appears to be in the correct order of magnitude.

Free-Floating Characteristics

Aileron floating angle.- Typical oscillograph records of the free-floating characteristics of the three ailerons through the Mach number range are presented in figure 14. These records are traces of aileron position against time at a given Mach number and from these traces floating angle, frequency, and amplitude of aileron motion were determined. Due to faulty operation of the timer mechanism in the oscillograph, timer lines were not recorded on some of the records. These records were read by using timer lines from other records since all records were taken at the same film speed. The error thus introduced is believed to be small.

Figure 15 is a plot of average floating angle against Mach number, and these angles are in good agreement with the trim angles indicated by the static hinge moments (figs. 6, 7, and 8). Floating angle does not vary with Mach number until the critical speed of the wing is exceeded. The difference in floating angle for the three ailerons at a given subcritical Mach number has been attributed to model asymmetry. Above M_{cr} there is a large variation in floating angle for the aileron with $t = 0$. This variation in floating angle is to be expected in the speed range when the hinge moments are unstable. The variation with time of the position of the aileron with $t = 0$ is very rough at subcritical speeds in comparison with the blunted trailing-edge ailerons due to a relatively low value of C_{hs} .

Aileron oscillations.- A high-frequency, low-amplitude aileron oscillation with only one degree of freedom was encountered for all three ailerons. These oscillations will be referred to herein as buzz. It should be noted that these oscillations never developed into large-amplitude oscillations as has sometimes been encountered, as shown in references 11 and 12. Buzz was spasmodic when first encountered but as the speed increased it became a sustained oscillation with a range of aileron movement of about 2° . The Mach number at which buzz first occurred varied for each aileron (fig. 16). The aileron with $t = 1.0$ buzzed at subcritical speeds and the ailerons with $t = 0$ and $t = 0.5$ did not buzz until the critical speed of the wing ($M_{cr} = 0.87$) had been exceeded. The motion of the aileron with $t = 0.5$ was the least severe. At the high test Mach numbers, above $M = 1.05$, all three ailerons experienced irregular high-amplitude oscillations - indicating that severe disturbing forces were present.

Results from tests of the aileron with $t = 1.0$ with increased moment of inertia show that the increase in moment of inertia did not eliminate buzz, but it did decrease the frequency (fig. 16).

Methods for computing buzz frequency are presented in references 5 and 6. These empirical theories predict buzz somewhere in the speed range from M_{cr} to $M = 1.00$. In order to compare data from the present investigation with these empirical theories, a Mach number in the predictable speed range for buzz was chosen. A comparison of the experimental and calculated frequencies at $M = 0.95$ is given in table II.

In order to compute buzz frequencies from references 5 and 6 it was necessary to make certain basic assumptions concerning flow conditions around the wing, since no shadowgraph data were available. For reference 5, the critical Mach number was taken as $M = 0.87$ from the drag data of reference 3, and the minimum pressure point was assumed to be located at 50 percent of the chord. In computing buzz frequency by the method of reference 6, the shock wave was assumed to be located at 70 percent of the chord after a study of the pressure-distribution data of reference 13. Due to these basic assumptions, only qualitative results can be expected.

CONCLUSIONS

Comparative tests of aileron trailing-edge-thickness modifications at subsonic and transonic speeds on a 42.7° sweptback circular-arc wing indicated the following conclusions:

1. Increasing the aileron trailing-edge thickness results in a negative shift in the aileron hinge-moment parameters $C_{h\delta}$ and $C_{h\alpha}$.
2. The reversal of $C_{h\delta}$ at supercritical speeds was eliminated by increased aileron trailing-edge thickness.
3. Buzz was least severe for the aileron having a trailing-edge thickness of one half the hinge-line thickness and occurred over a larger speed range for the aileron having a trailing-edge thickness equal to the thickness at the hinge line.

4. Buzz frequency was decreased by increasing the moment of inertia of the aileron.

Langley Aeronautical Laboratory
National Advisory Committee for Aeronautics
Langley Air Force Base, Va.

REFERENCES

1. Turner, Thomas R., Lockwood, Vernard E., and Vogler, Raymond D.: Preliminary Investigation of Various Ailerons on a 42° Sweptback Wing for Lateral Control at Transonic Speeds. NACA RM L8D21, 1948.
2. Sandahl, Carl A.: Free-Flight Investigation at Transonic and Supersonic Speeds of the Rolling Effectiveness of a 42.7° Sweptback Wing Having Partial-Span Ailerons. NACA RM L8E25, 1948.
3. Turner, Thomas R., Lockwood, Vernard E., and Vogler, Raymond D.: Aerodynamic Characteristics at Subsonic and Transonic Speeds of a 42.7° Sweptback Wing Model Having an Aileron with Finite Trailing-Edge Thickness. NACA RM L8K02, 1949.
4. Sandahl, Carl A.: Free-Flight Investigation at Transonic and Supersonic Speeds of the Rolling Effectiveness of Several Aileron Configurations on a Tapered Wing Having 42.7° Sweepback. NACA RM L8K23, 1949.
5. Erickson, Albert L., and Stephenson, Jack D.: A Suggested Method of Analyzing for Transonic Flutter of Control Surfaces Based on Available Experimental Evidence. NACA RM A7F30, 1947.
6. Smilg, Benjamin: The Prevention of Aileron Oscillations at Transonic Airspeeds. AAF TR No. 5530, Materiel Command, Army Air Forces, Dec. 24, 1946.
7. Schneiter, Leslie E., and Ziff, Howard L.: Preliminary Investigation of Spoiler Lateral Control on a 42° Sweptback Wing at Transonic Speeds. NACA RM L7F19, 1947.
8. Batson, A. S., Burge, C. H., and Skelton, W. C.: Experiments on the Effect of Curvature of Surface and Thickness of Trailing Edge on Aileron Hinge Moments (Part III). Rep. No. 6188, British A.R.C., Oct. 20, 1942.
9. Sivells, James C., and Goin, Kenneth L.: Experimental and Calculated Hinge Moments of Two Ailerons on a 42.7° Sweptback Wing at a Mach Number of 1.9. NACA RM L8K24a, 1949.
10. Lowry, John G., Axelson, John A., and Johnson, Harold I.: Effects of Sweep on Controls. NACA RM L8A28c, 1948.

11. Brown, Harvey H., Rathert, George A., Jr., and Clousing, Lawrence A.: Flight-Test Measurements of Aileron Control Surface Behaviour at Supercritical Mach Numbers. NACA RM A7A15, 1947.
12. Crane, Harold L.: An Investigation of Aileron Oscillations at Transonic Speeds on NACA 23012 and 65-212 Airfoils by the Wing-Flow Method. NACA RM L8K29, 1948.
13. Liepmann, Hans Wolfgang: Investigations of the Interaction of Boundary Layer and Shock Waves in Transonic Flow. Tech. Rep. No. 5688, ATI No. 34705, Air Materiel Command, U. S. Air Force, Feb. 9, 1948.

TABLE I

AILERON MOMENT OF INERTIA

Aileron thickness ratio, t	I (lb-in. sec ⁻²)
0	8.33×10^{-7}
.5	9.77×10^{-7}
1.0, I_1	9.46×10^{-7}
1.0, I_2	3.25×10^{-6}
1.0, I_3	2.08×10^{-5}

NACA

TABLE II

COMPARISON AT $M = 0.95$ OF BUZZ FREQUENCIES COMPUTED
BY REFERENCE ANALYSES WITH EXPERIMENTAL FREQUENCIES

Aileron thickness ratio, t	Buzz frequency (cps)		
	Experimental	Reference 5	Reference 6
0	310	226	290
.5	300($M = 1.0$)	220	290
1.0, I_1	310	241	290
1.0, I_2	125	192	247
1.0, I_3	50	No buzz	148

NACA

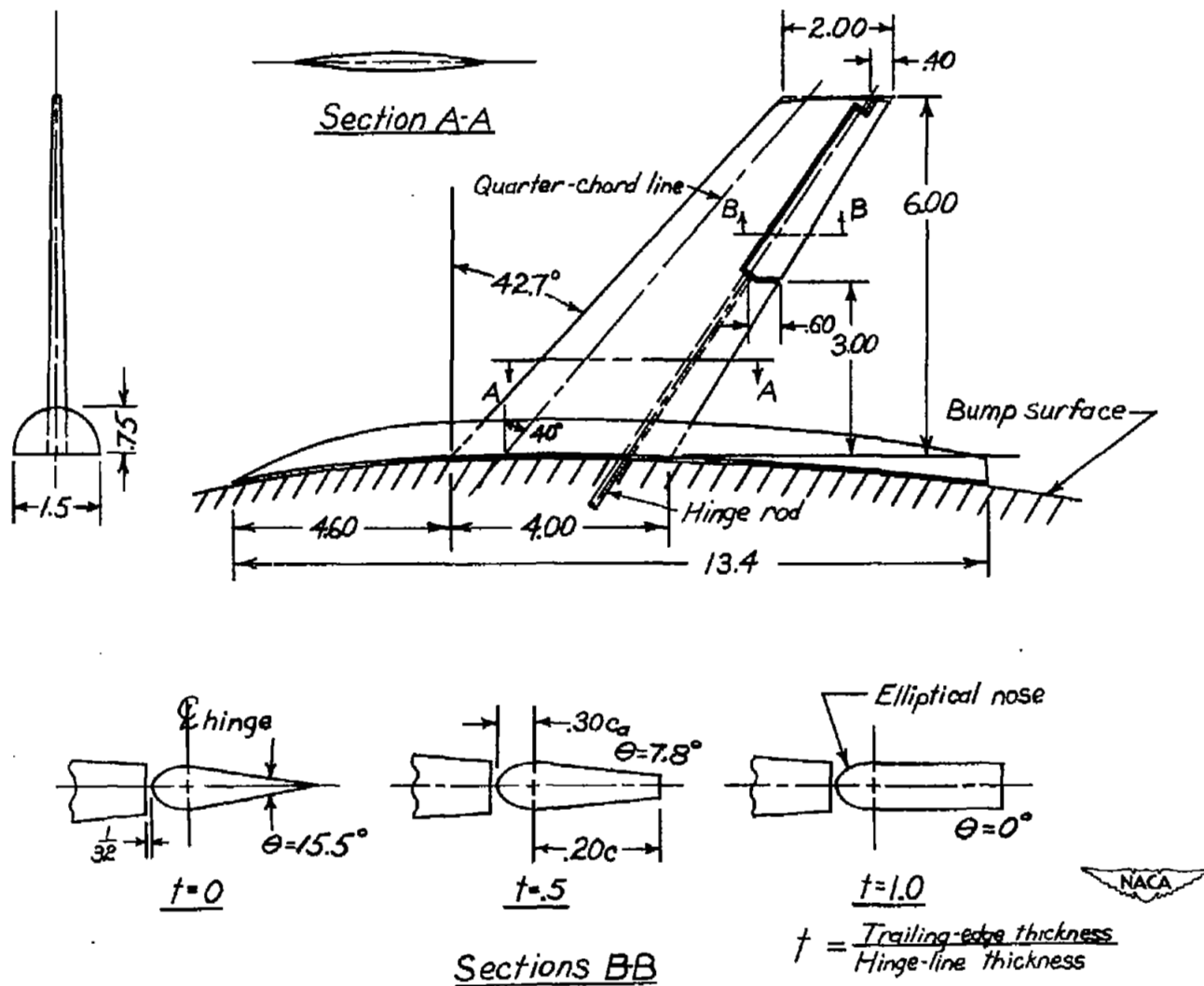


Figure 1.- The 42.7° sweptback wing-fuselage model. (All dimensions are in inches.)

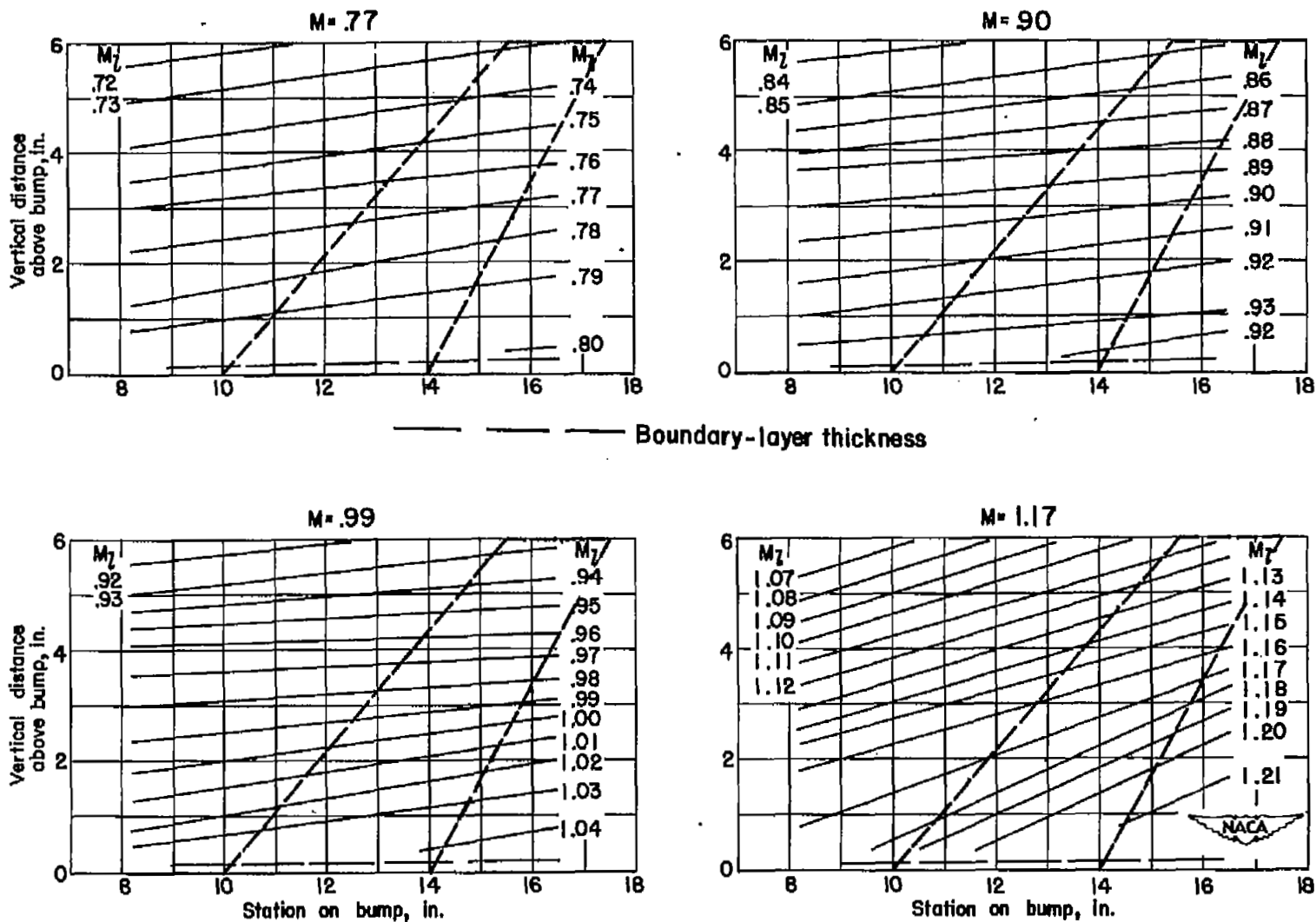


Figure 2.- Typical Mach number contours over transonic bump in region of model location.

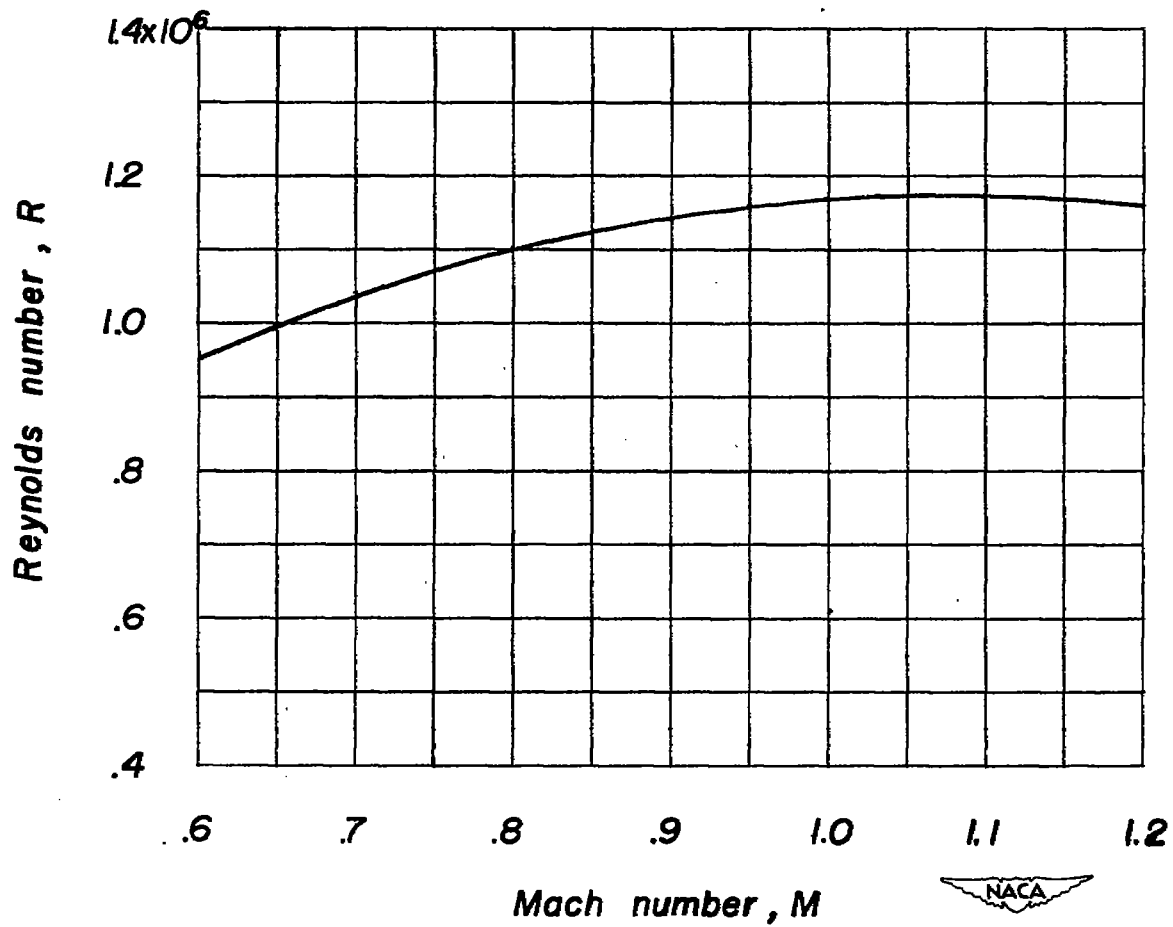


Figure 3.- Variation of average Reynolds number with Mach number.



Figure 4.- Photograph of the model as mounted on the bump in the Langley high-speed 7- by 10-foot tunnel. Wing tip braced.

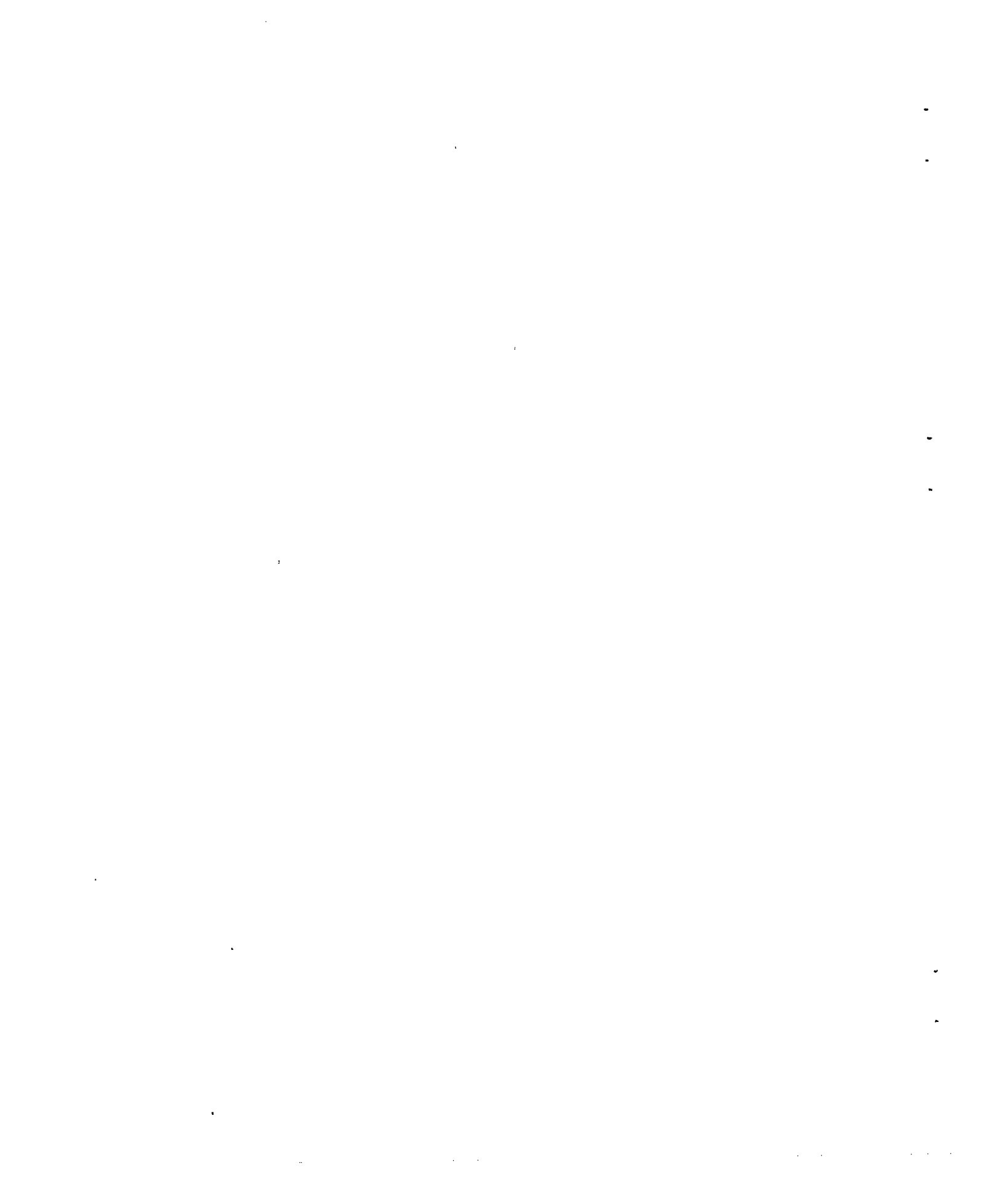
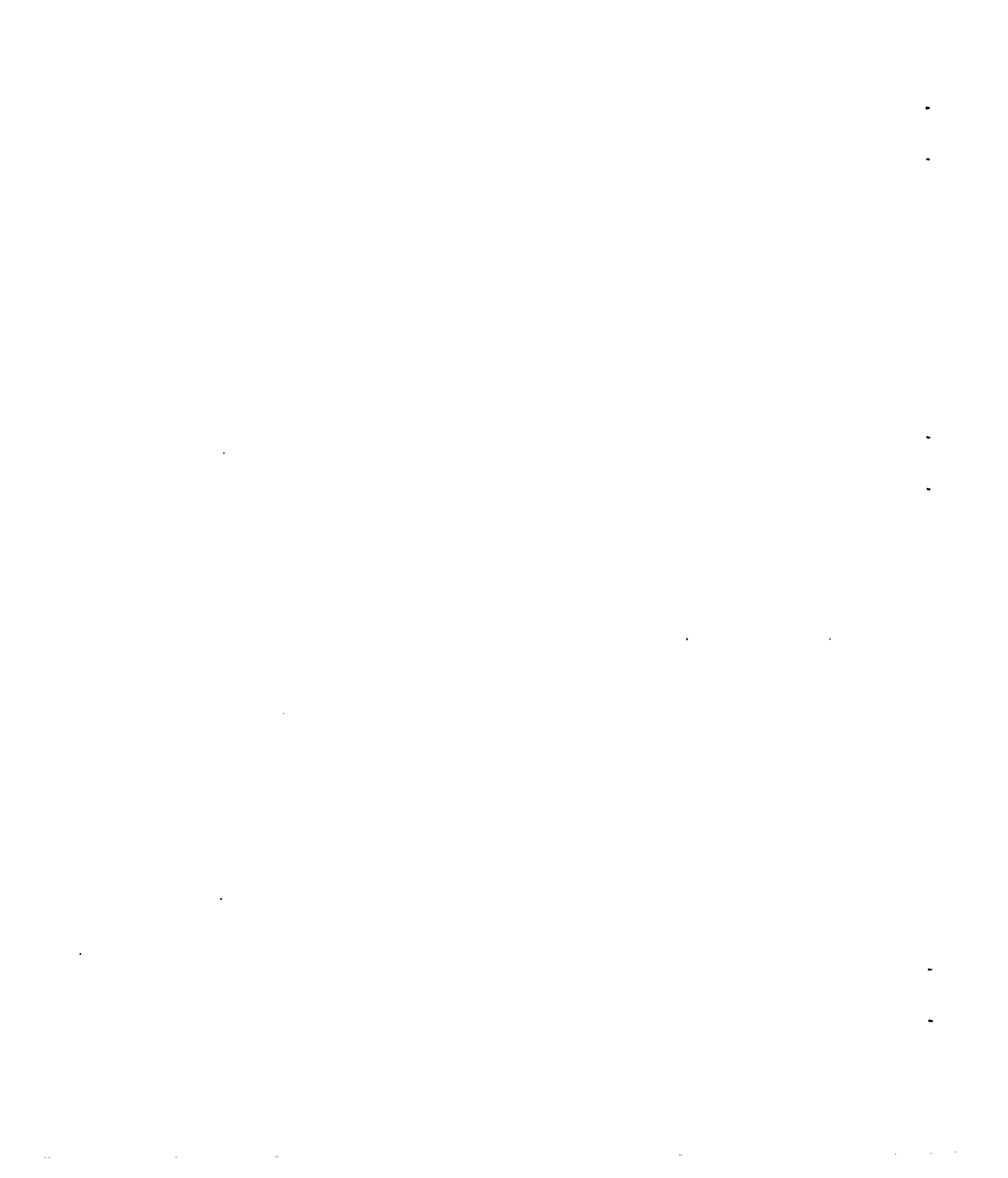




Figure 5.- Photograph of the model with wing-tip brace removed.



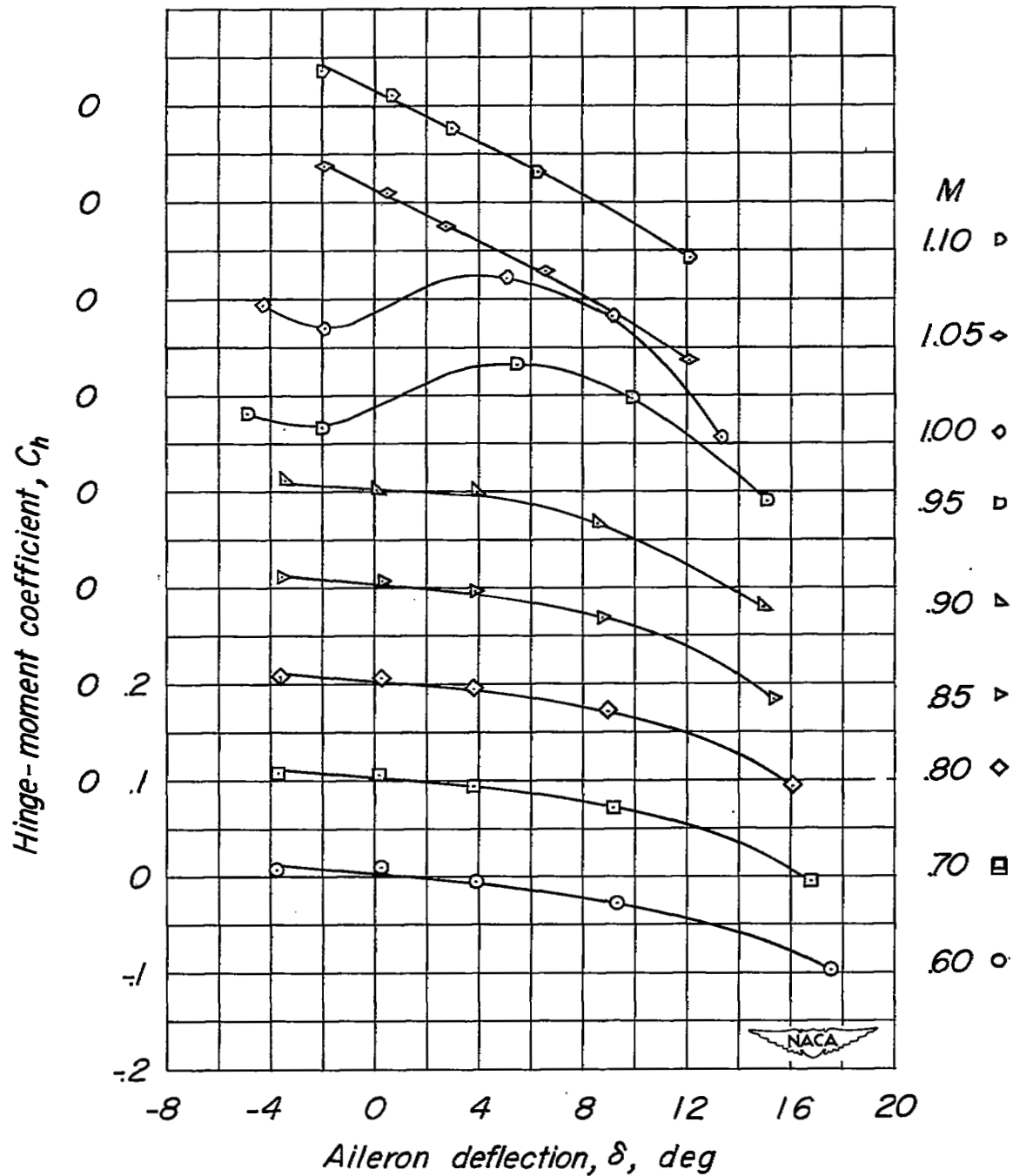


Figure 6.- Variation of hinge-moment coefficient with aileron deflection. $\alpha = 0^\circ$, $t = 0$.

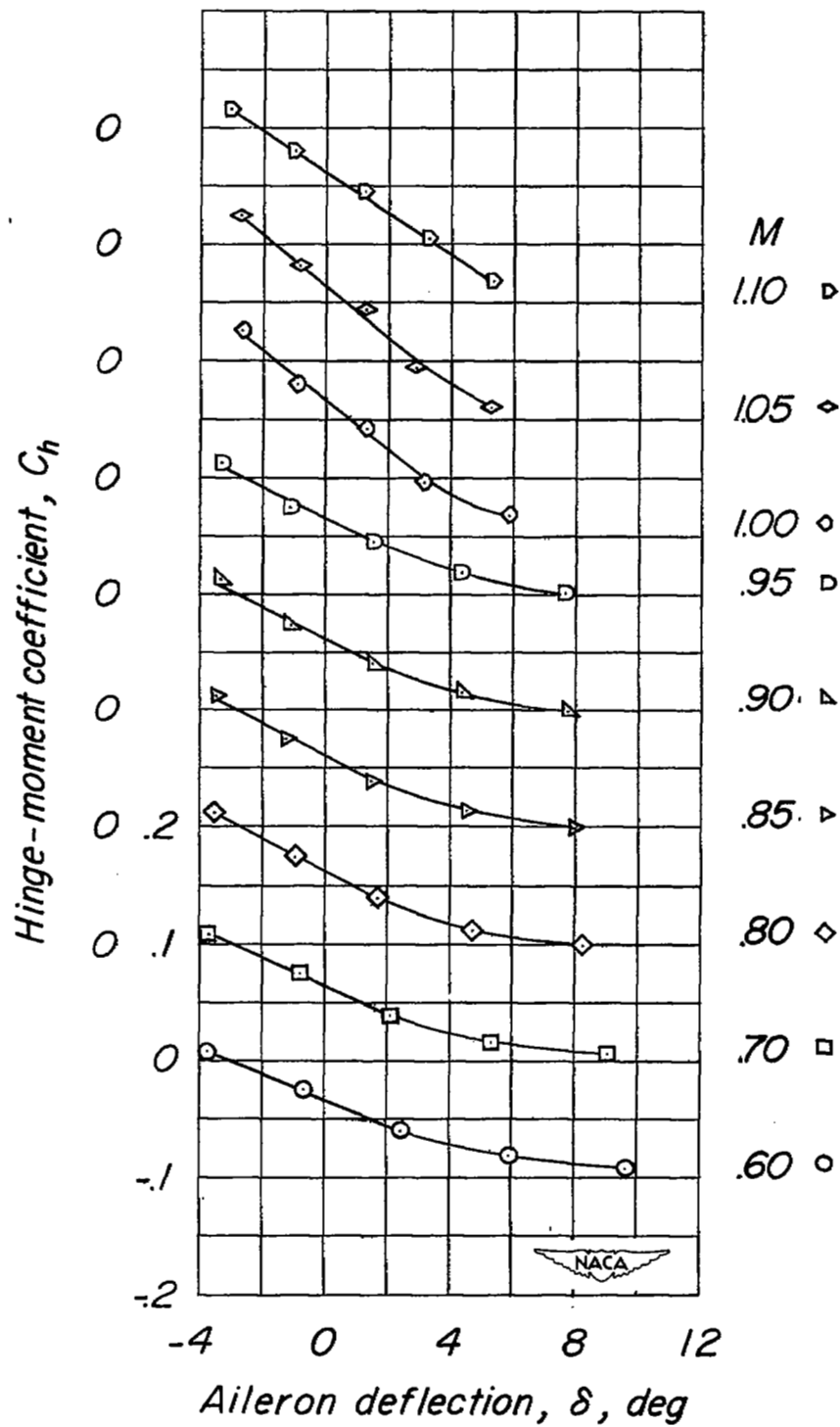


Figure 7.- Variation of hinge-moment coefficient with aileron deflection. $\alpha = 0^\circ$, $t = 0.5$.

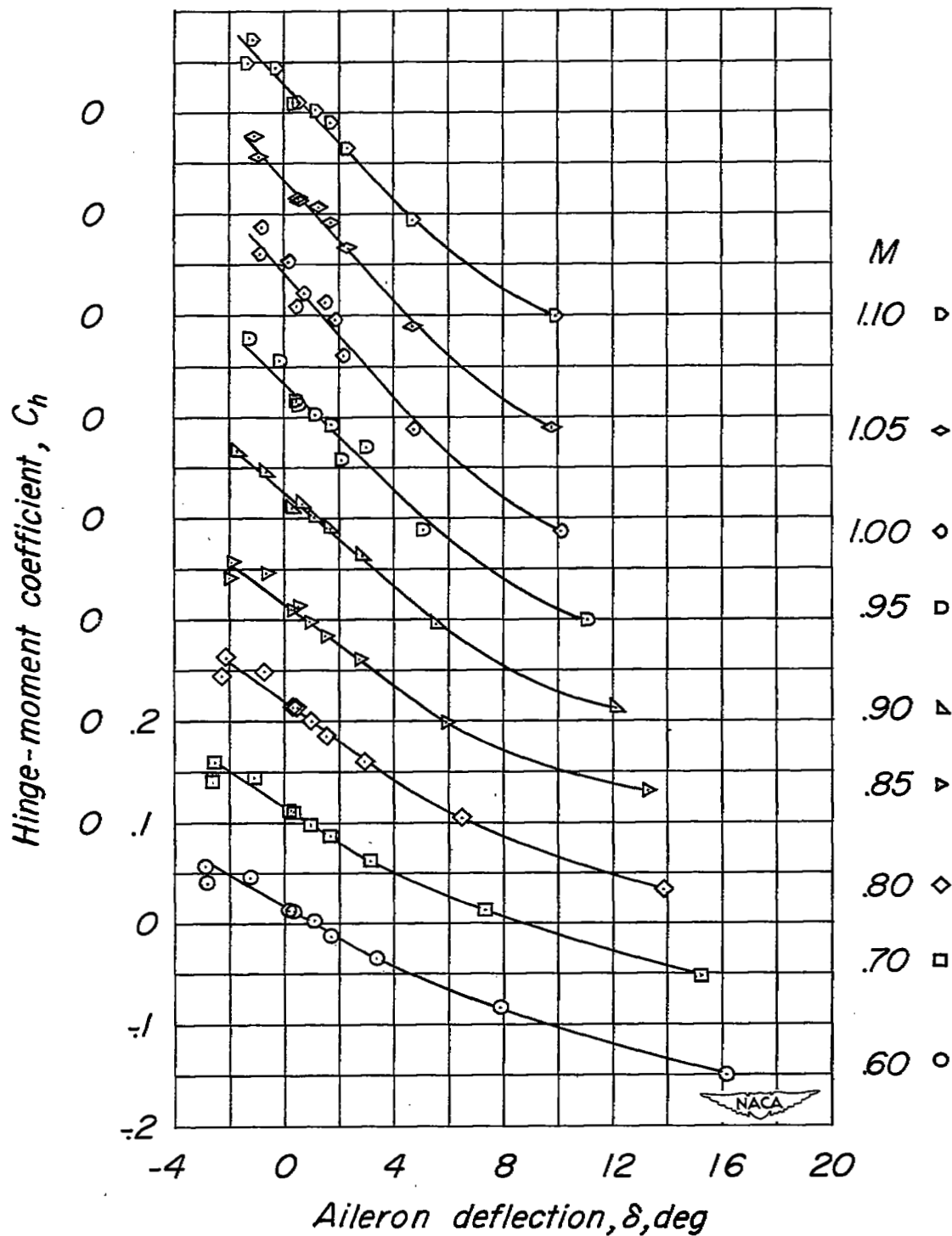


Figure 8.- Variation of hinge-moment coefficient with aileron deflection. $\alpha = 0^\circ$, $t = 1.0$.

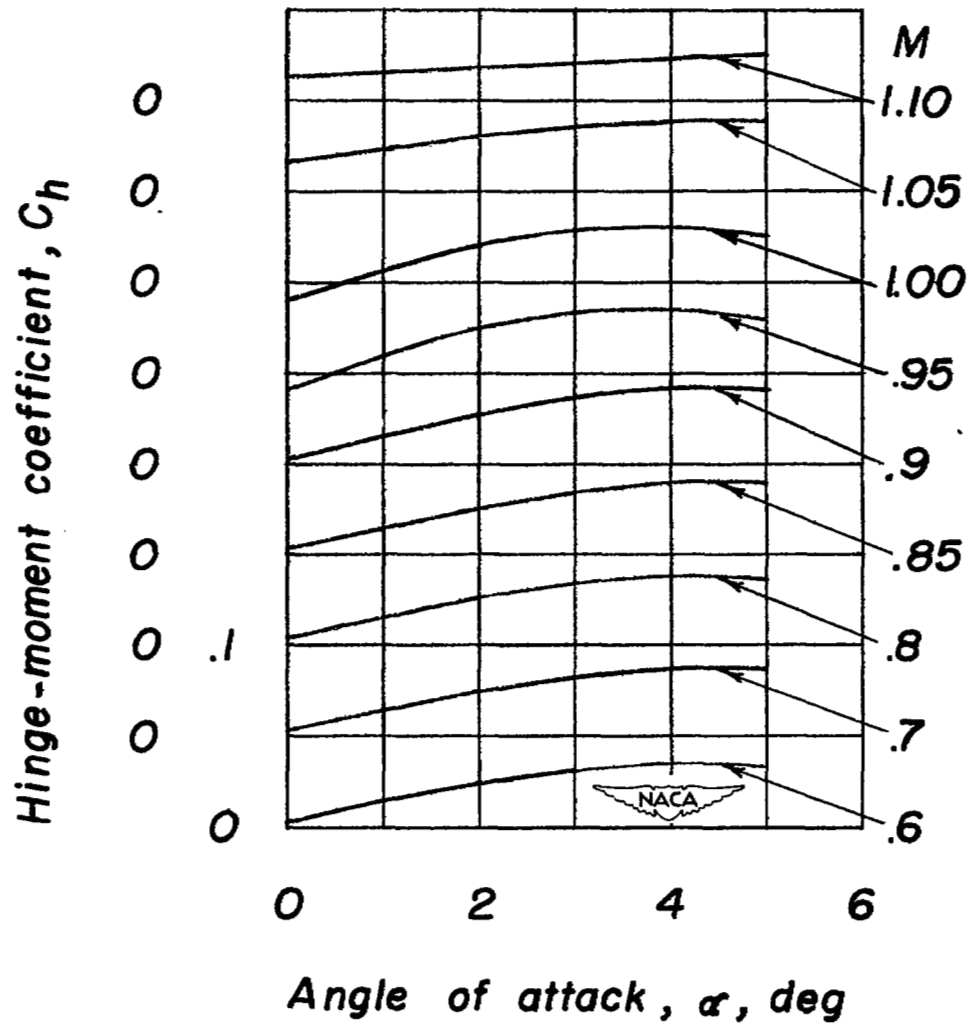


Figure 9. Variation of hinge-moment coefficient with angle of attack.
 $\delta = 0^\circ$, $t = 0$.

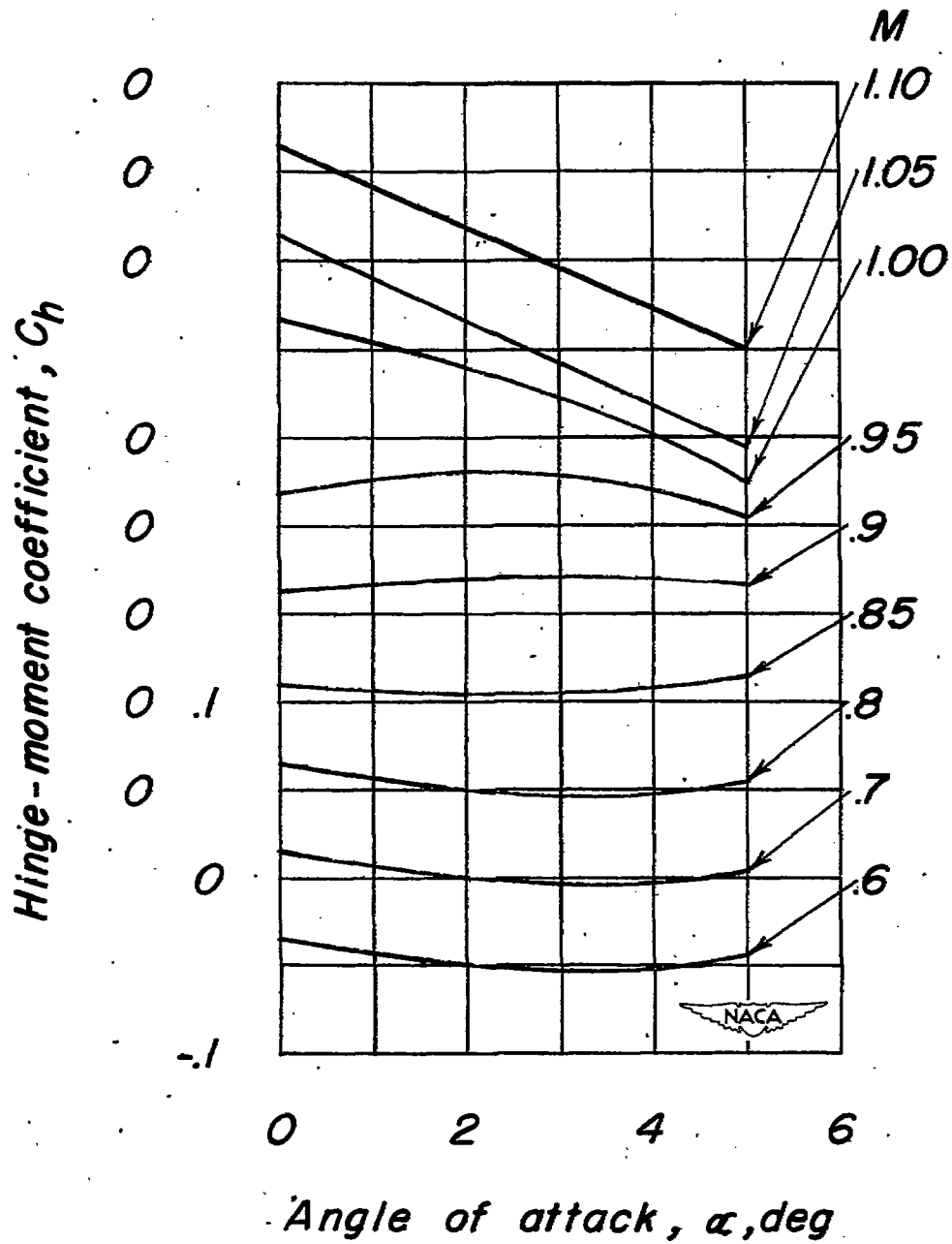


Figure 10.- Variation of hinge-moment coefficient with angle of attack.
 $\delta = 0^\circ$, $t = 0.5$.

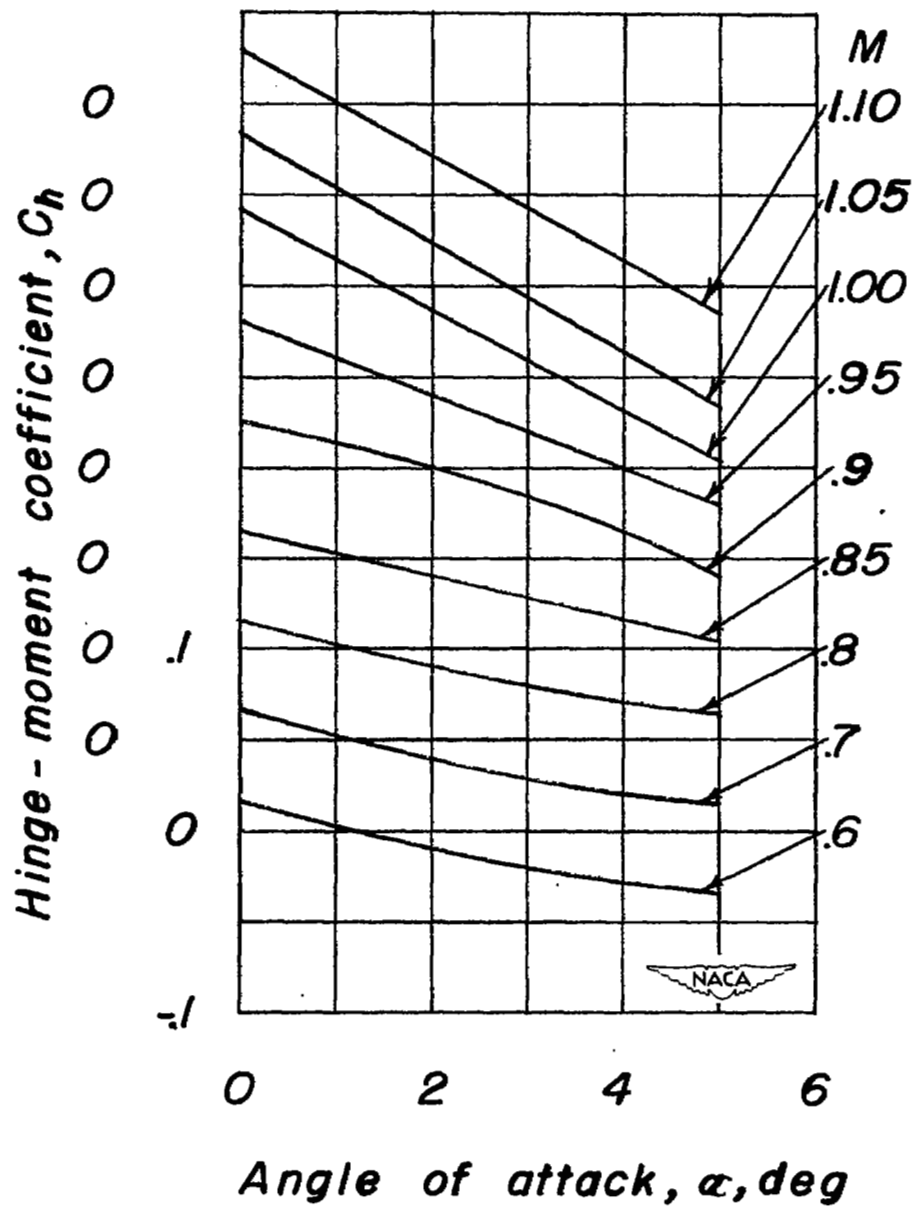


Figure 11.- Variation of hinge-moment coefficient with angle of attack.
 $\delta = 0^\circ$, $t = 1.0$.

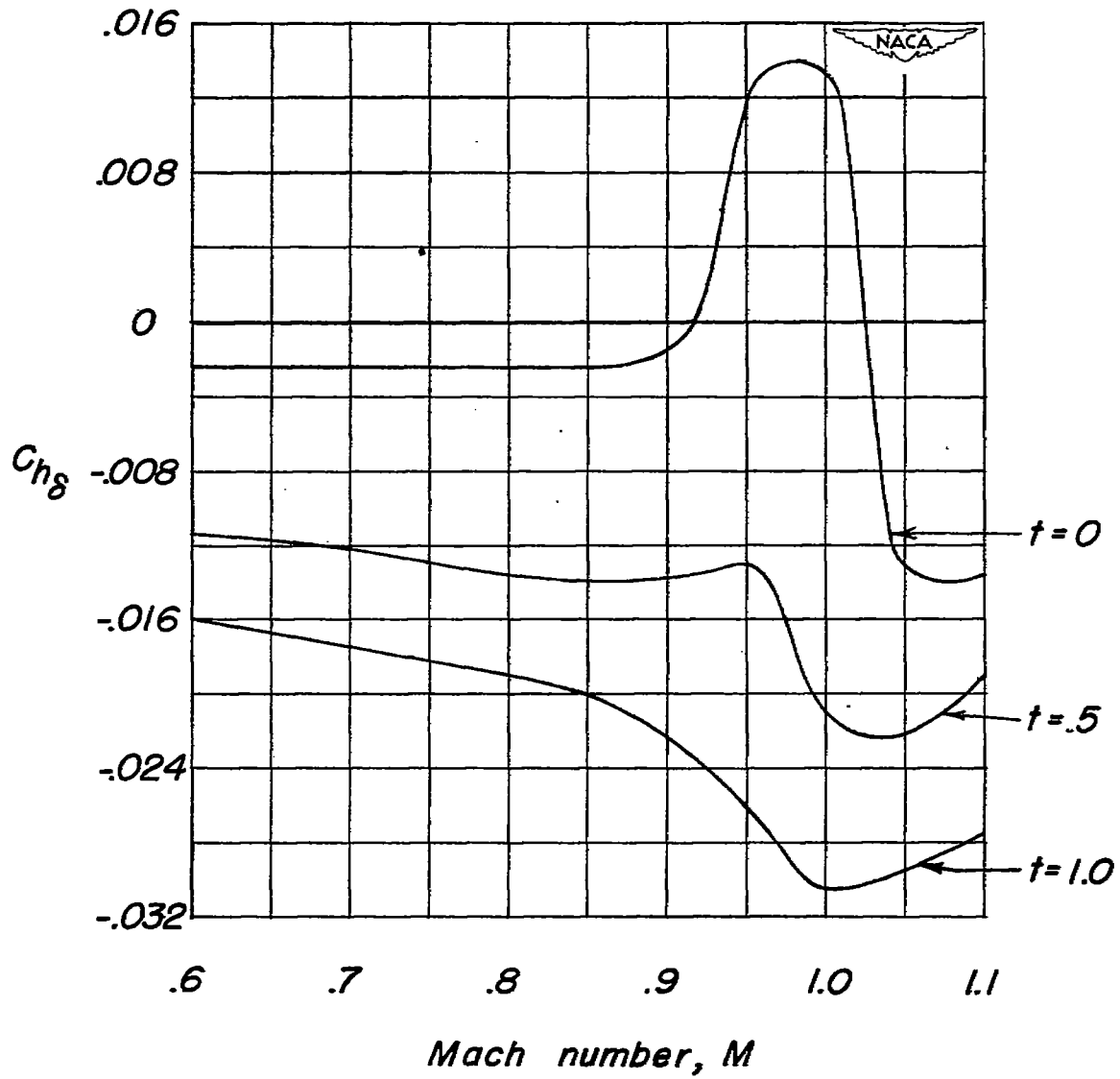


Figure 12.- Effect of Mach number on the hinge-moment parameter C_{h8} .

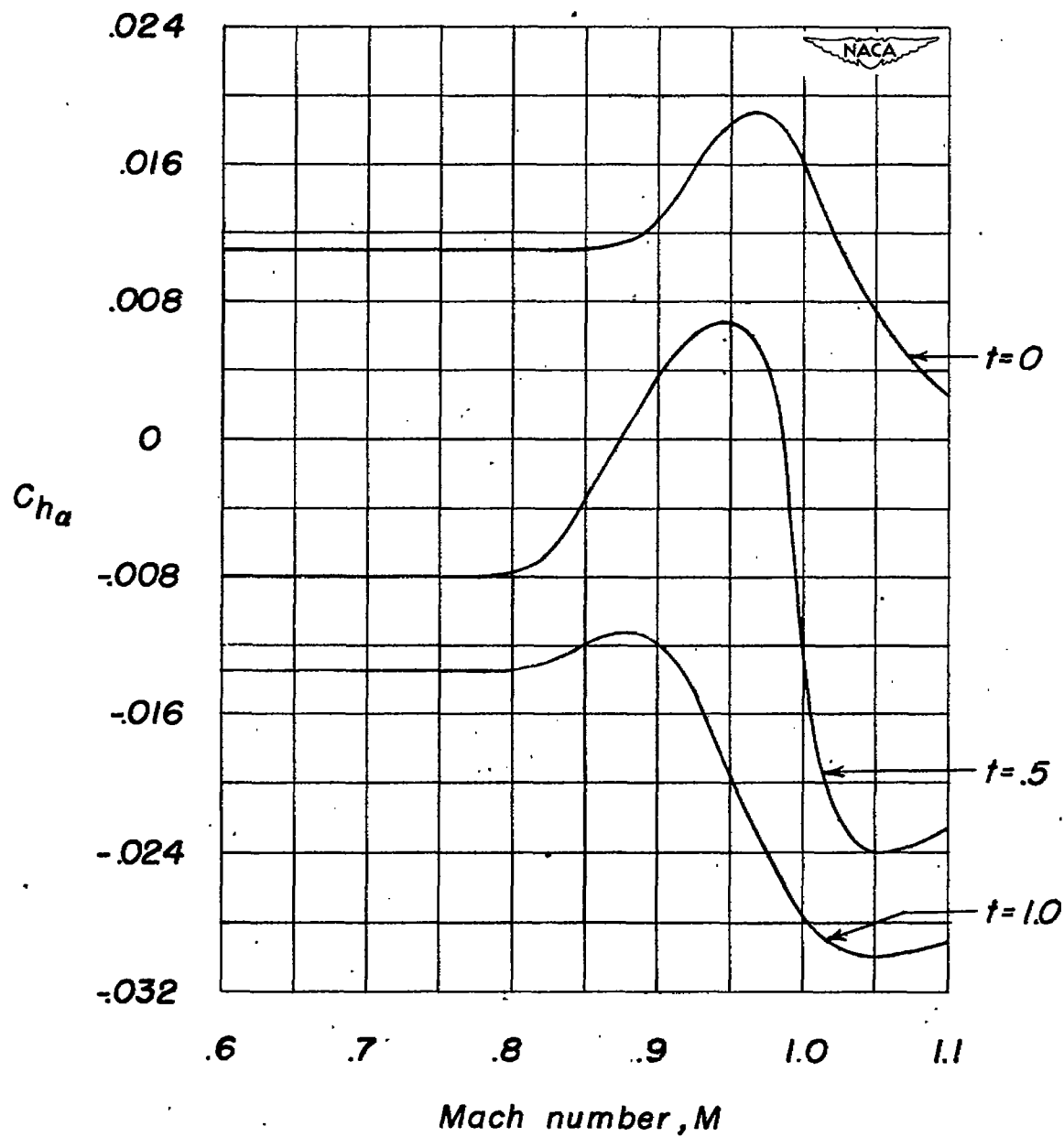
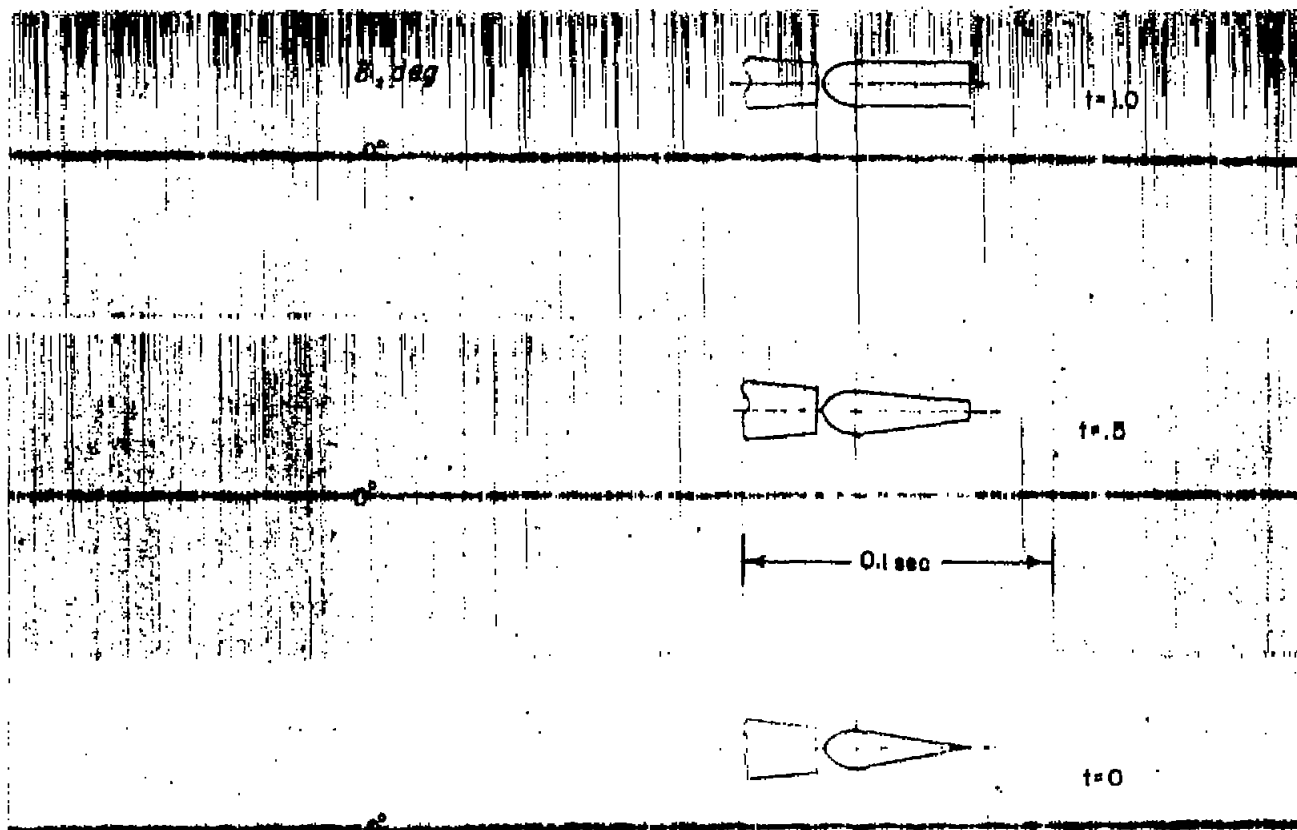
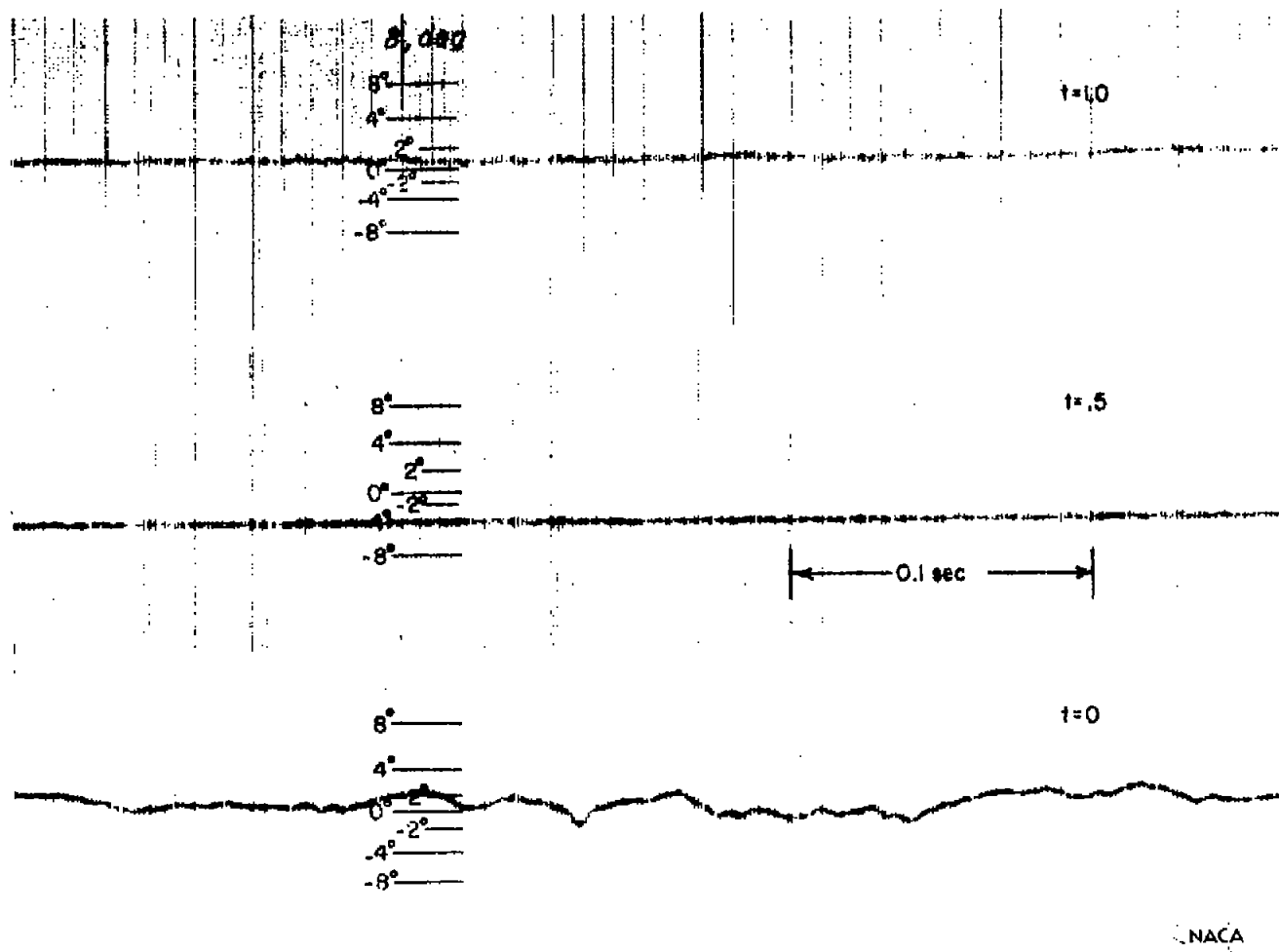


Figure 13.- Effect of Mach number on the hinge-moment parameter $C_{h\alpha}$.



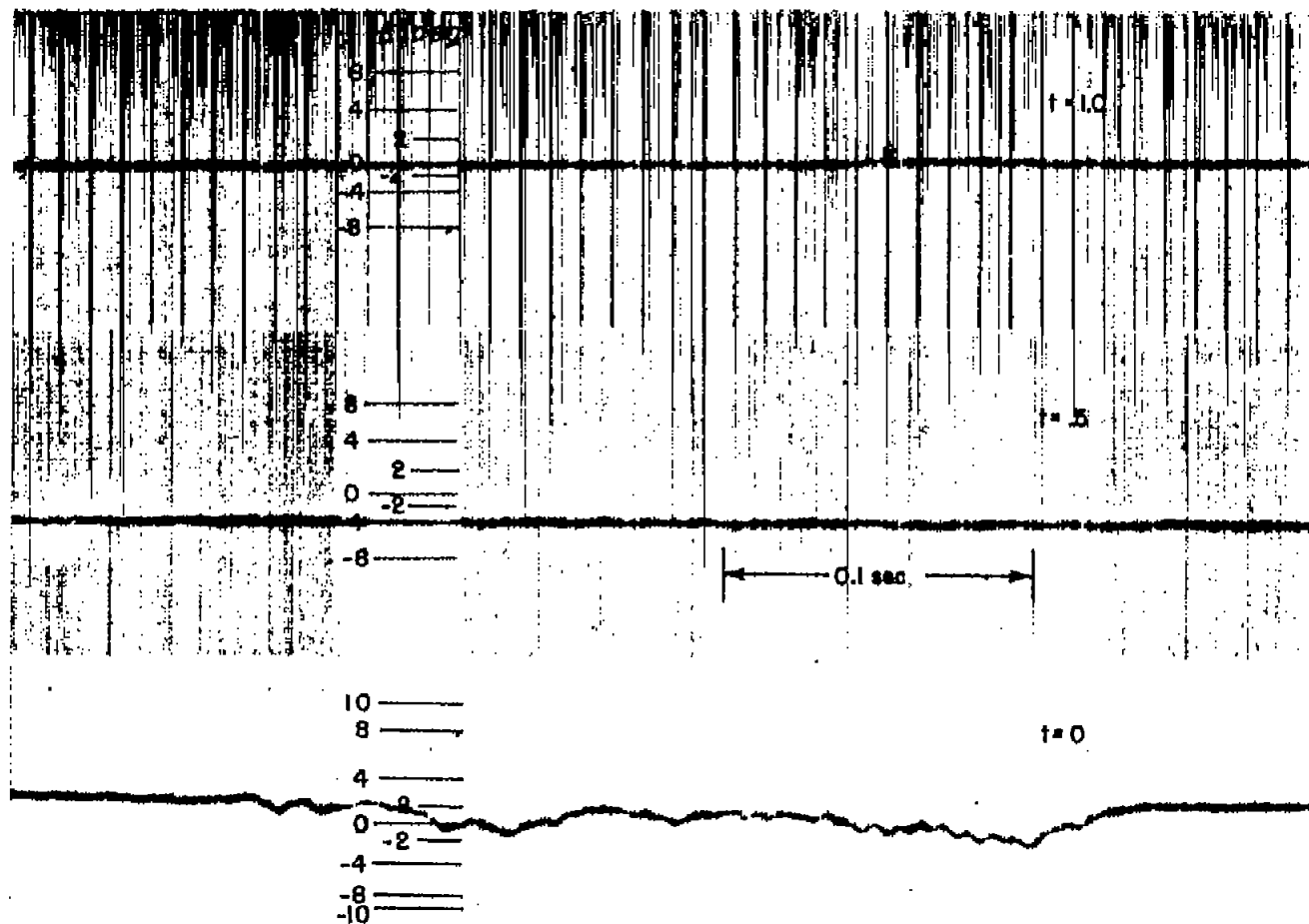
(a) Wind off.

Figure 14.- Records of aileron free-floating characteristics.



(b) $M = 0.60$.

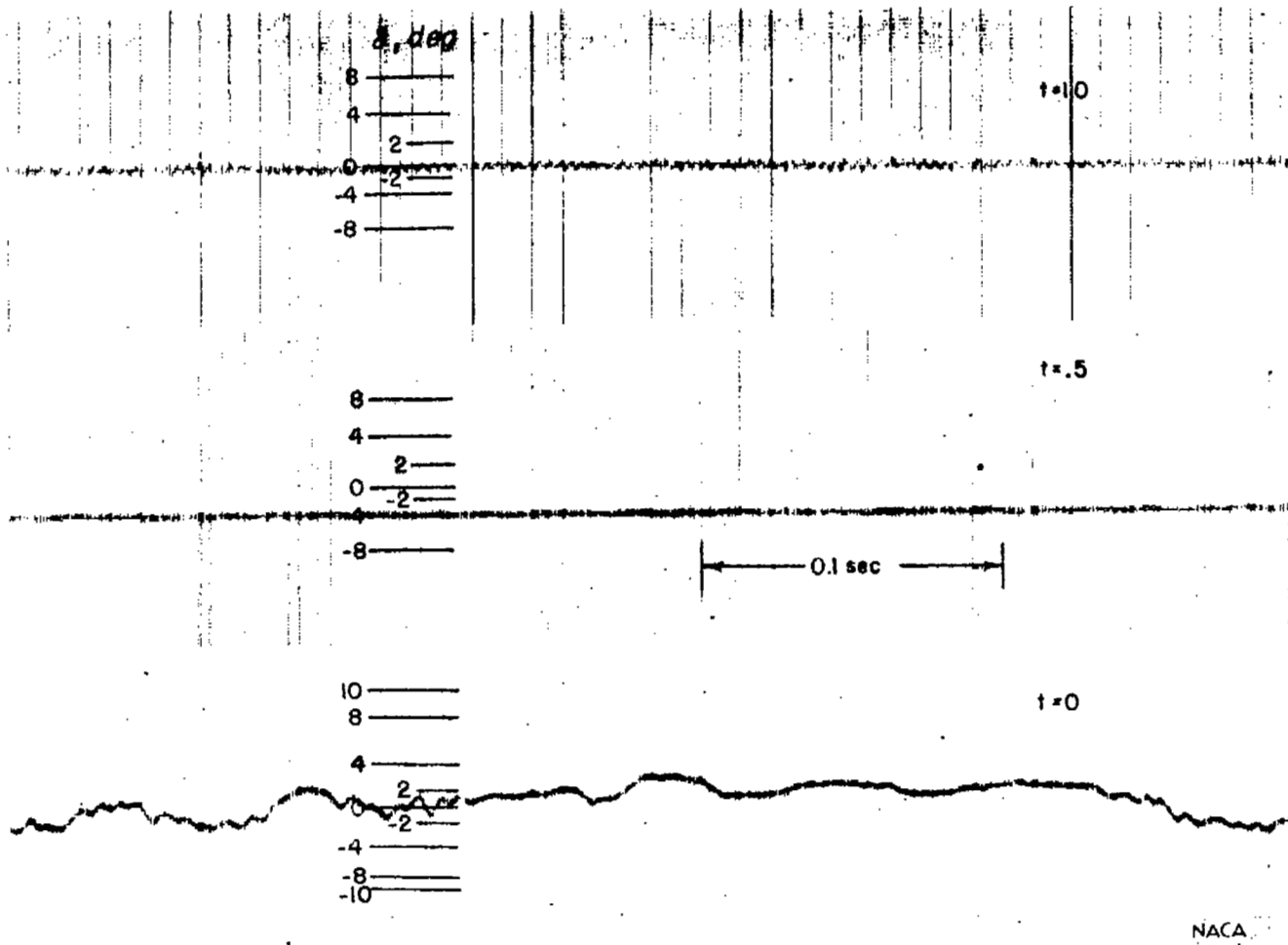
Figure 14.- Continued.



(c) $M = 0.70$.

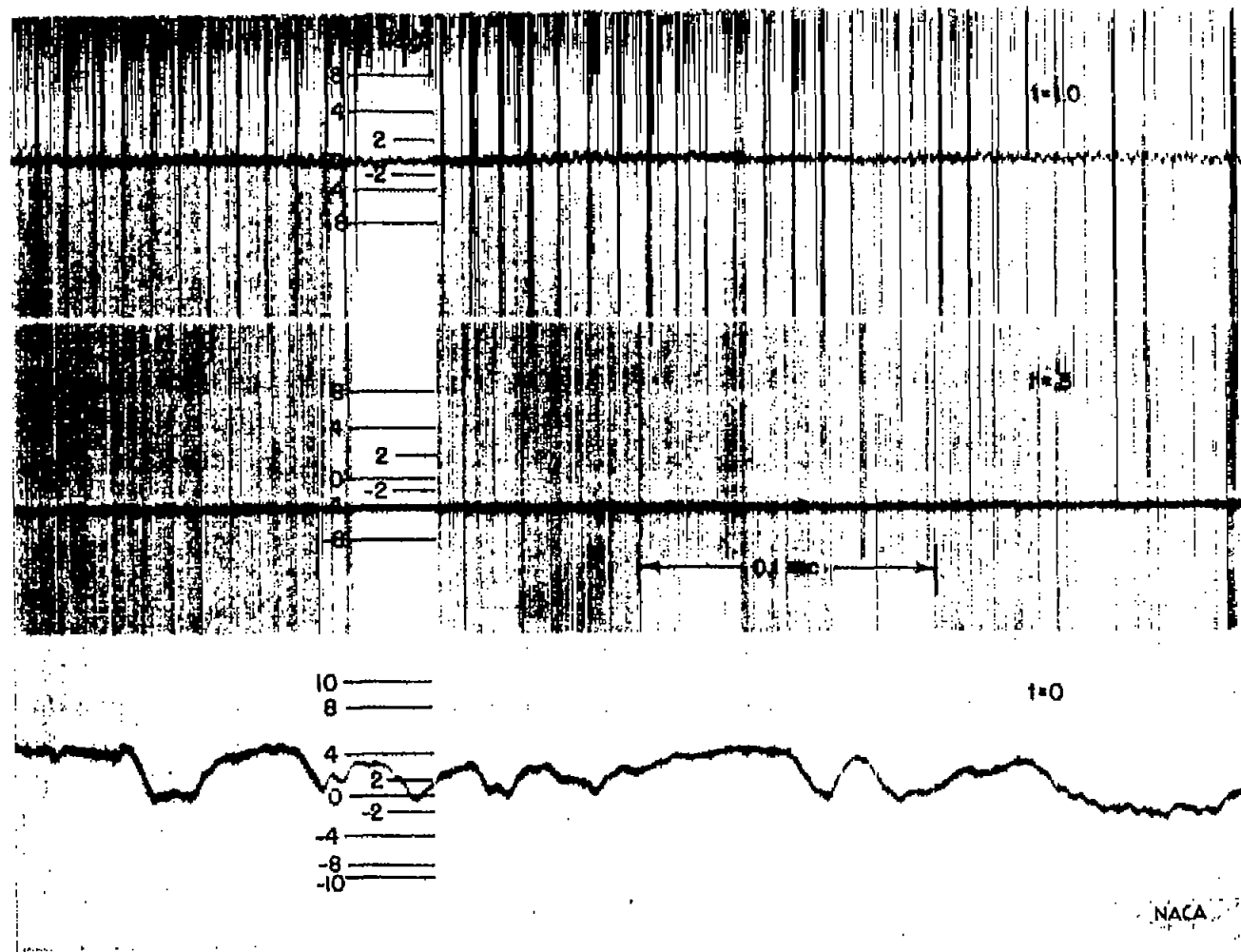
Figure 14.- Continued.

NACA



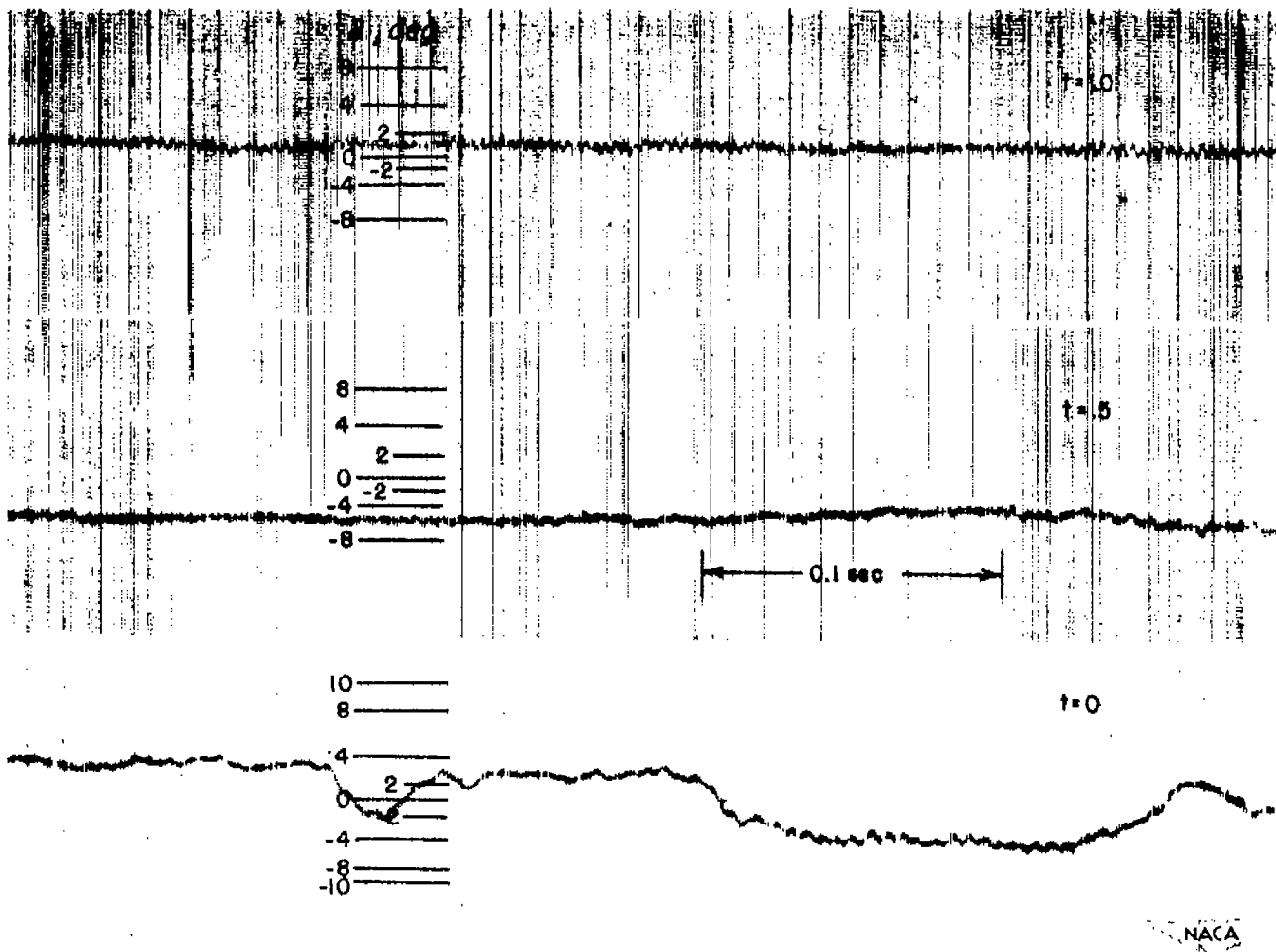
(d) $M = 0.80$.

Figure 14.- Continued.



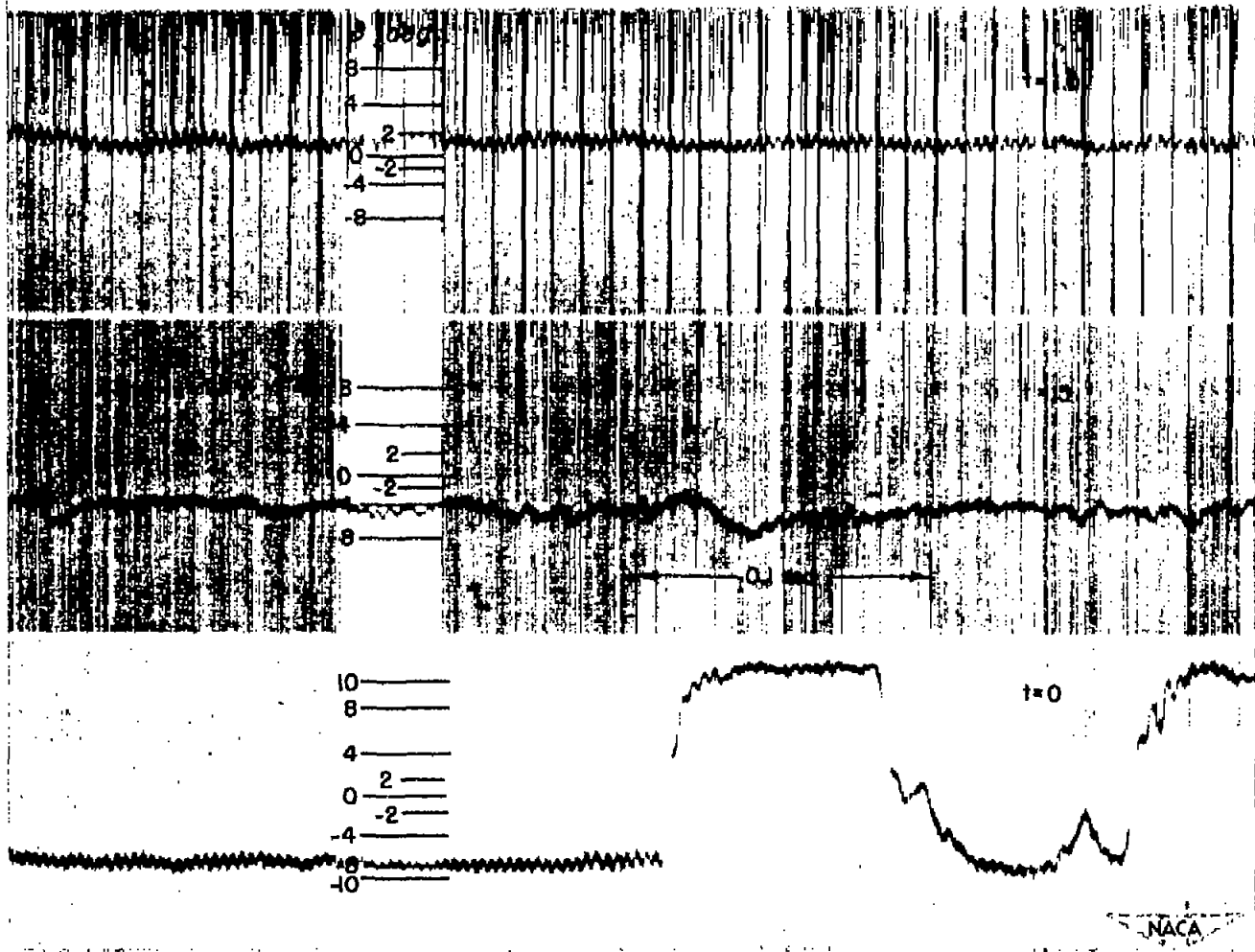
(e) $M = 0.85$.

Figure 14.- Continued.



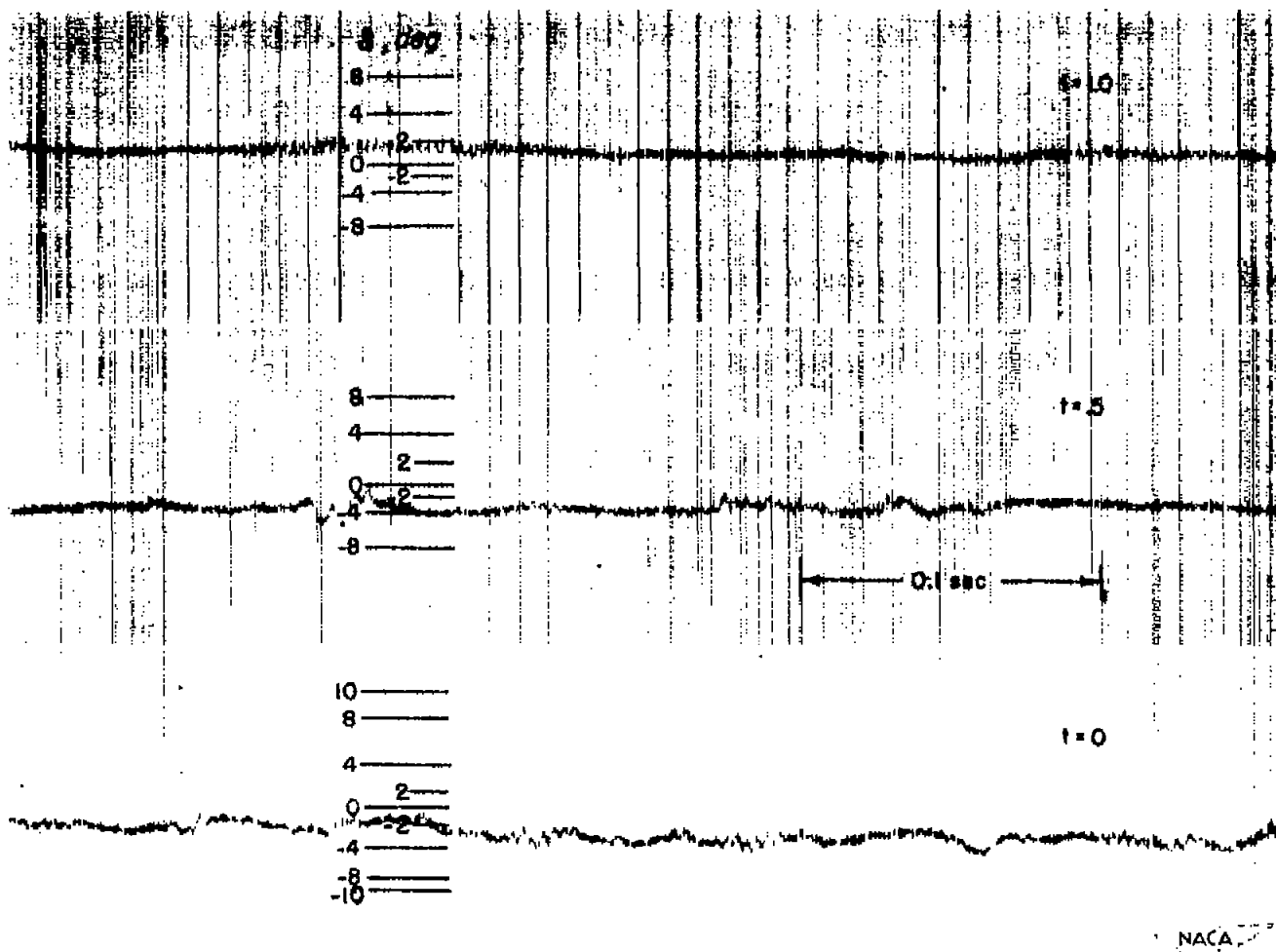
(f) $M = 0.90$.

Figure 14.- Continued.



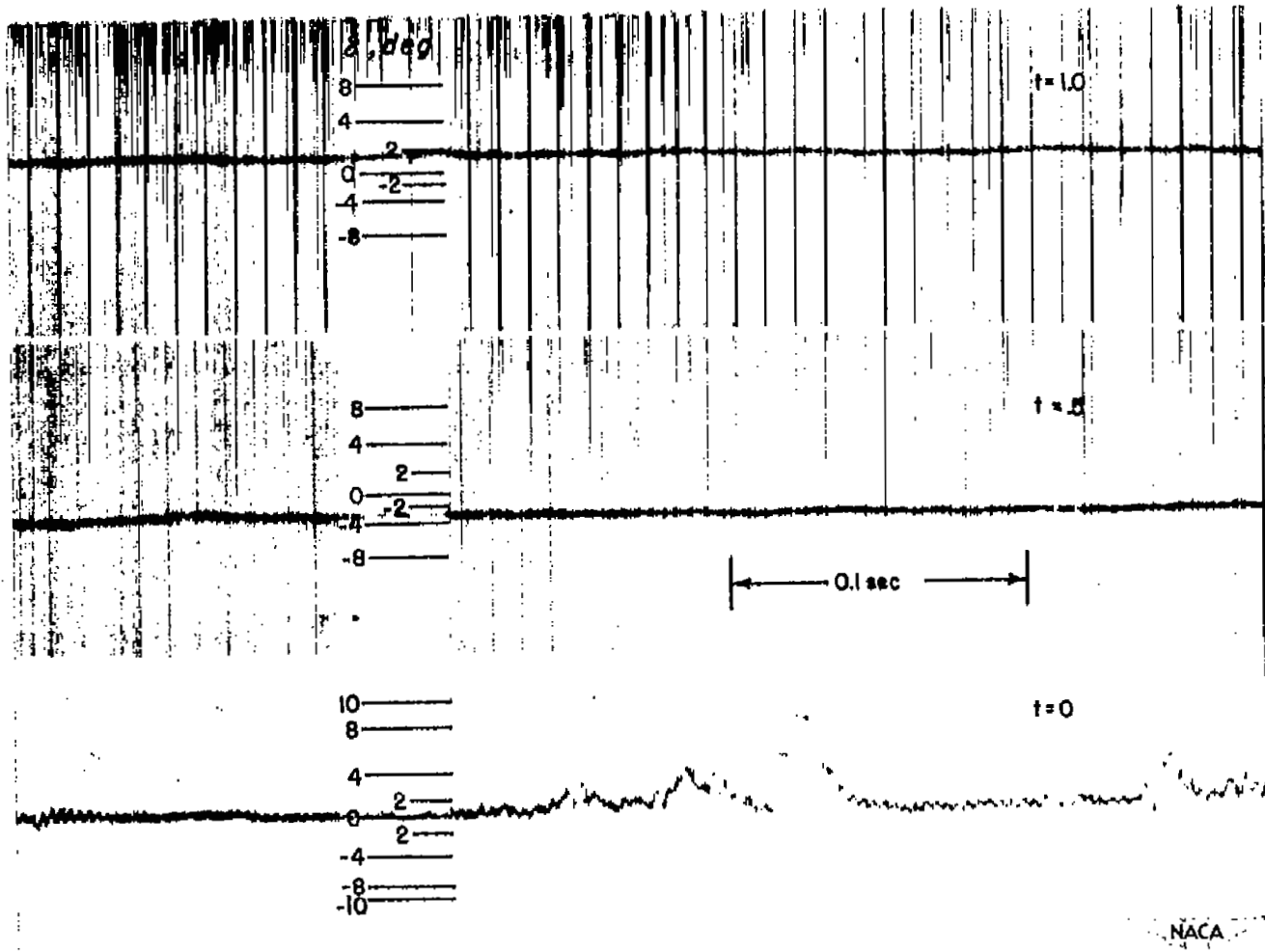
(g) $M = 0.95$.

Figure 14.- Continued.



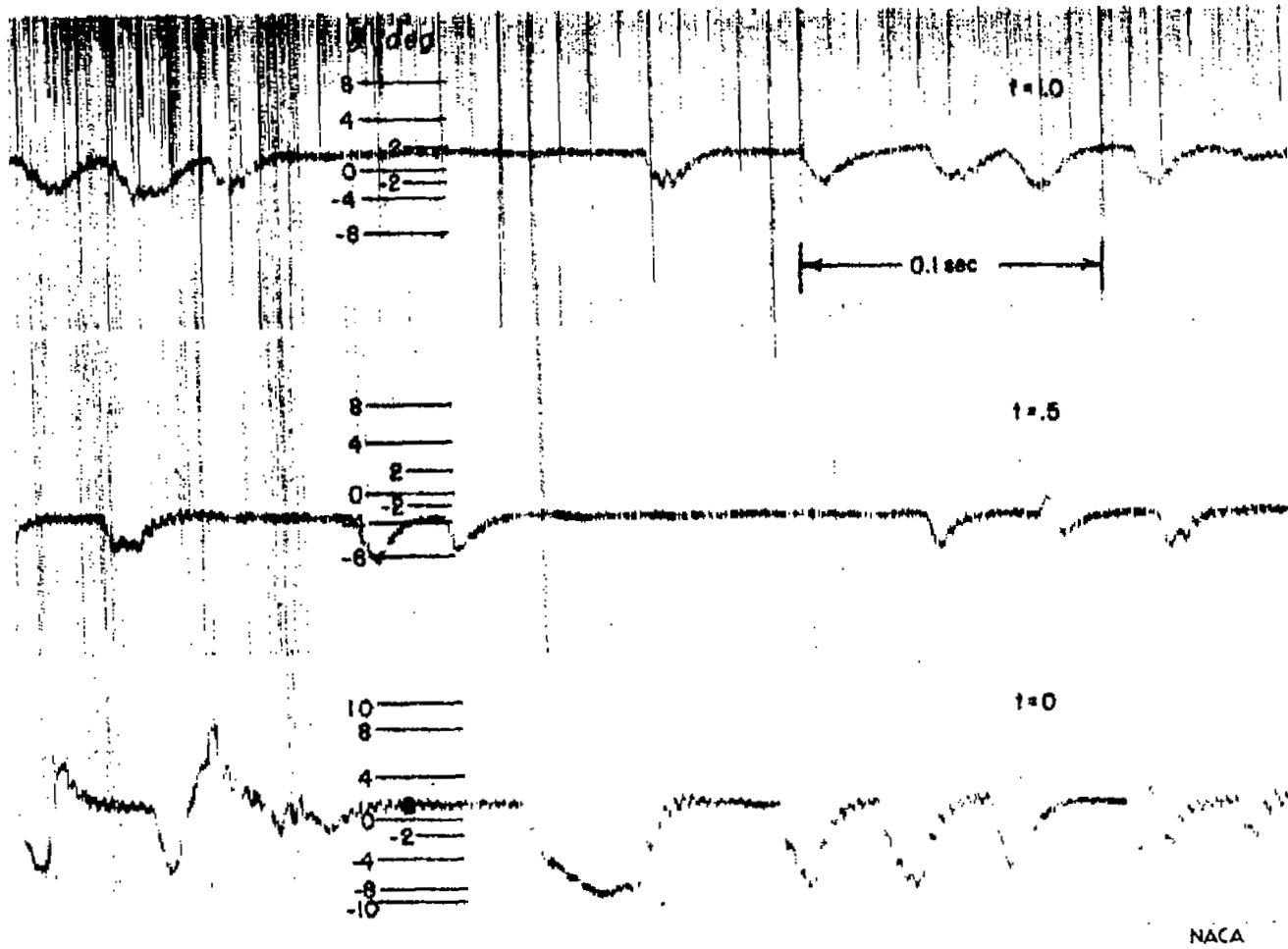
(h) $M = 1.00$.

Figure 14.- Continued.



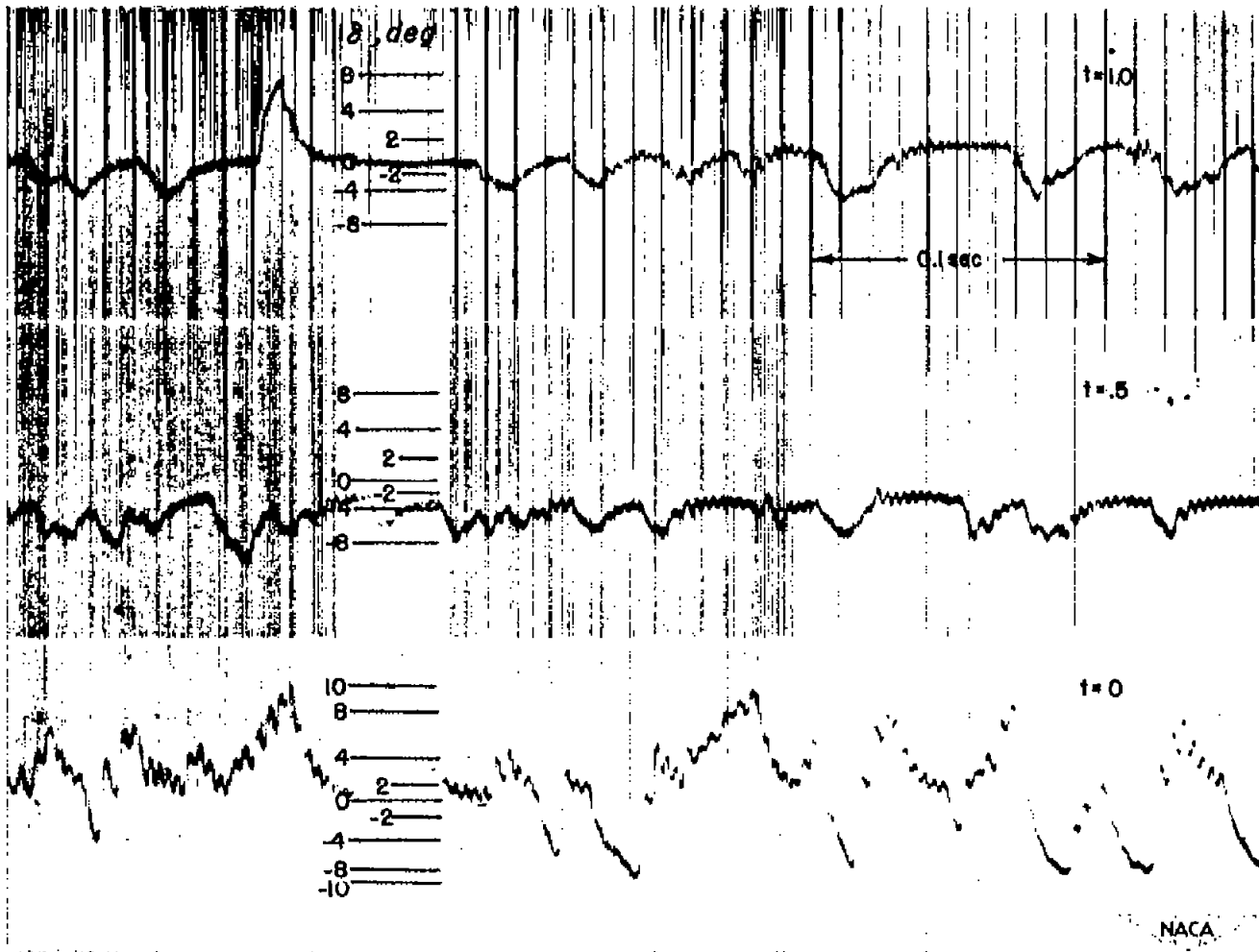
(1) $M = 1.05.$

Figure 14.- Continued.



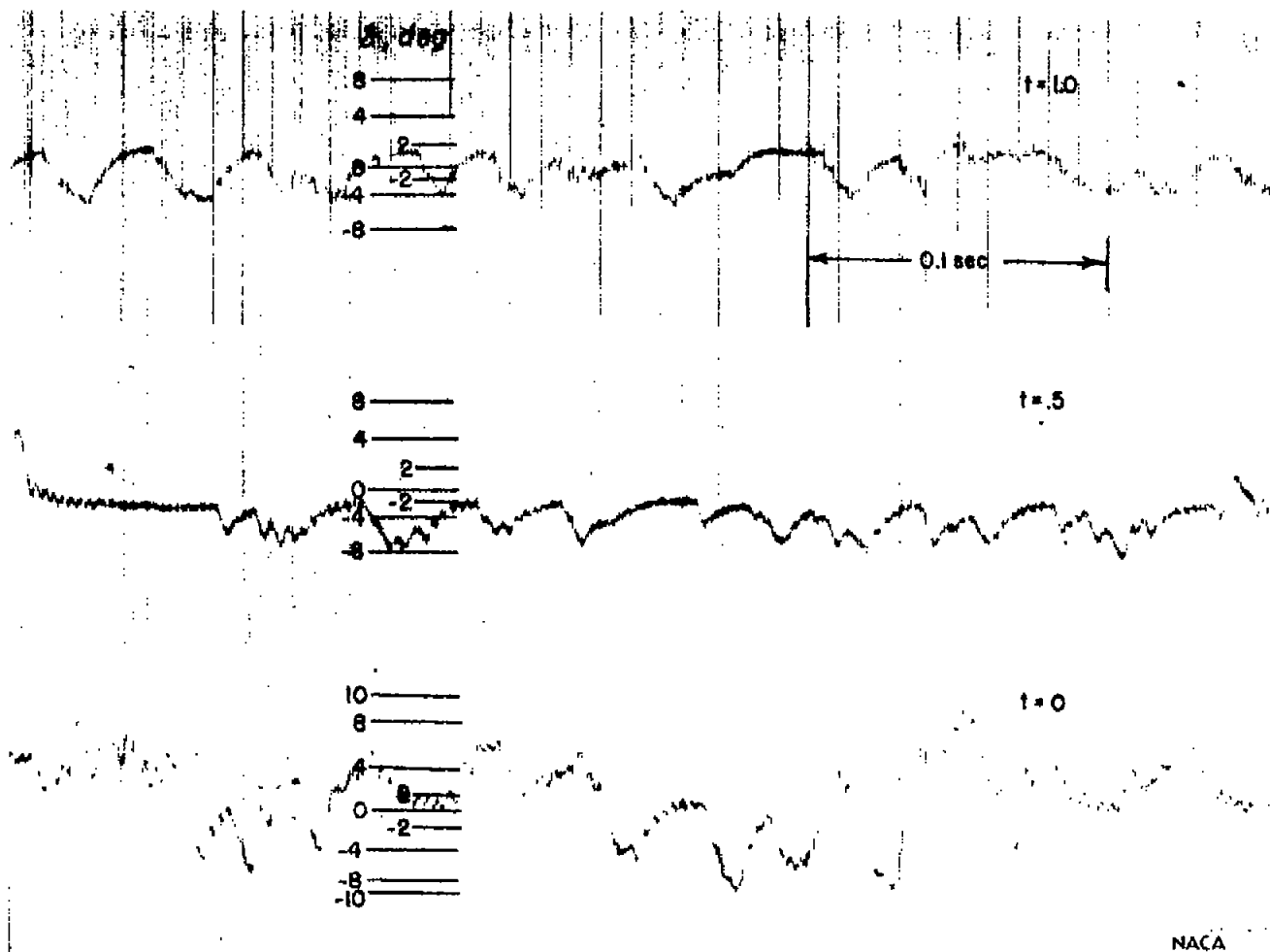
(j) $M = 1.10$.

Figure 14.- Continued.



(k) $M = 1.15$.

Figure 14.- Continued.



(2) $M = 1.175$.

Figure 14.- Concluded.

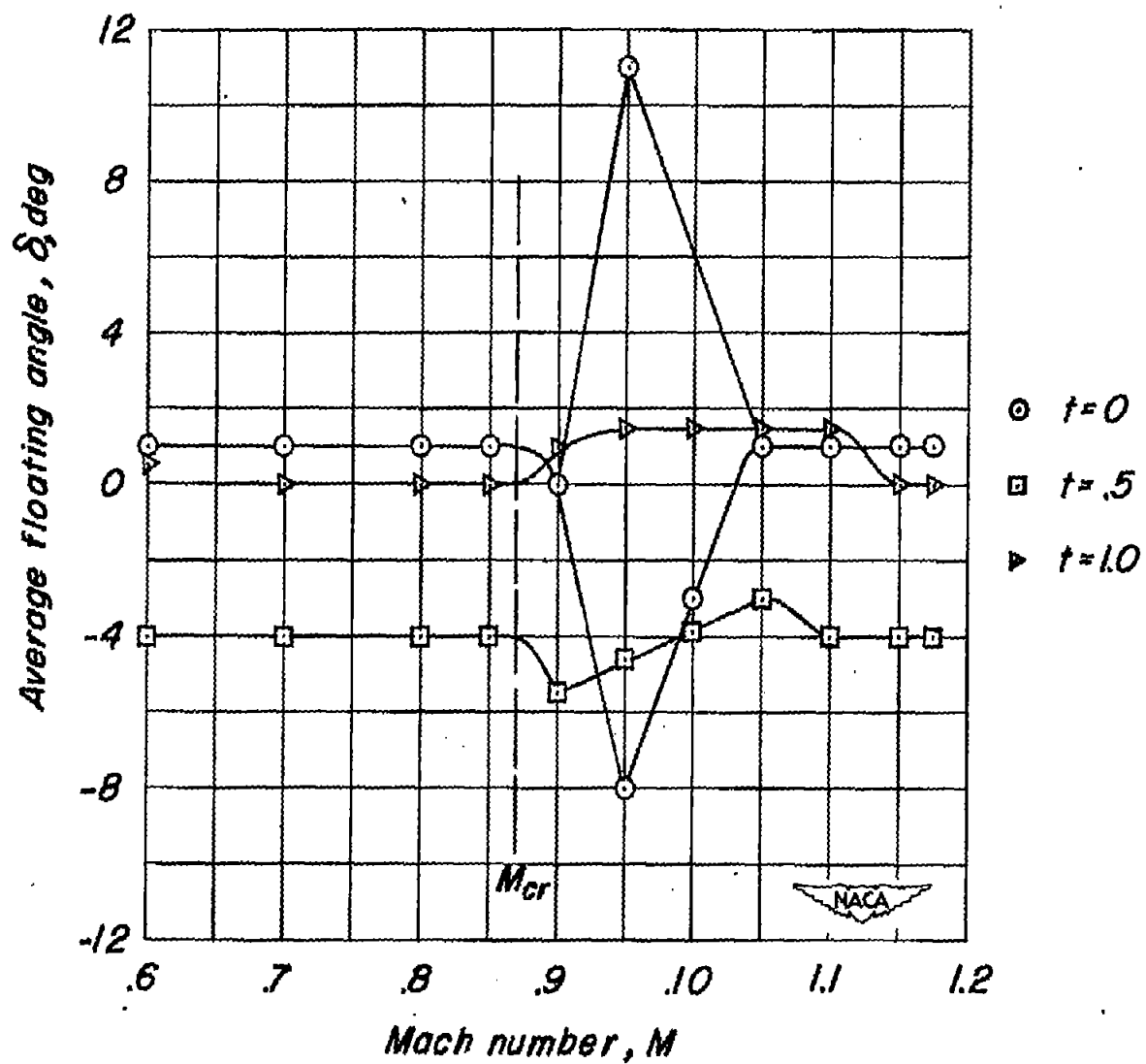


Figure 15.- Variation of average floating angle with Mach number.
 $\alpha = 0^\circ$.

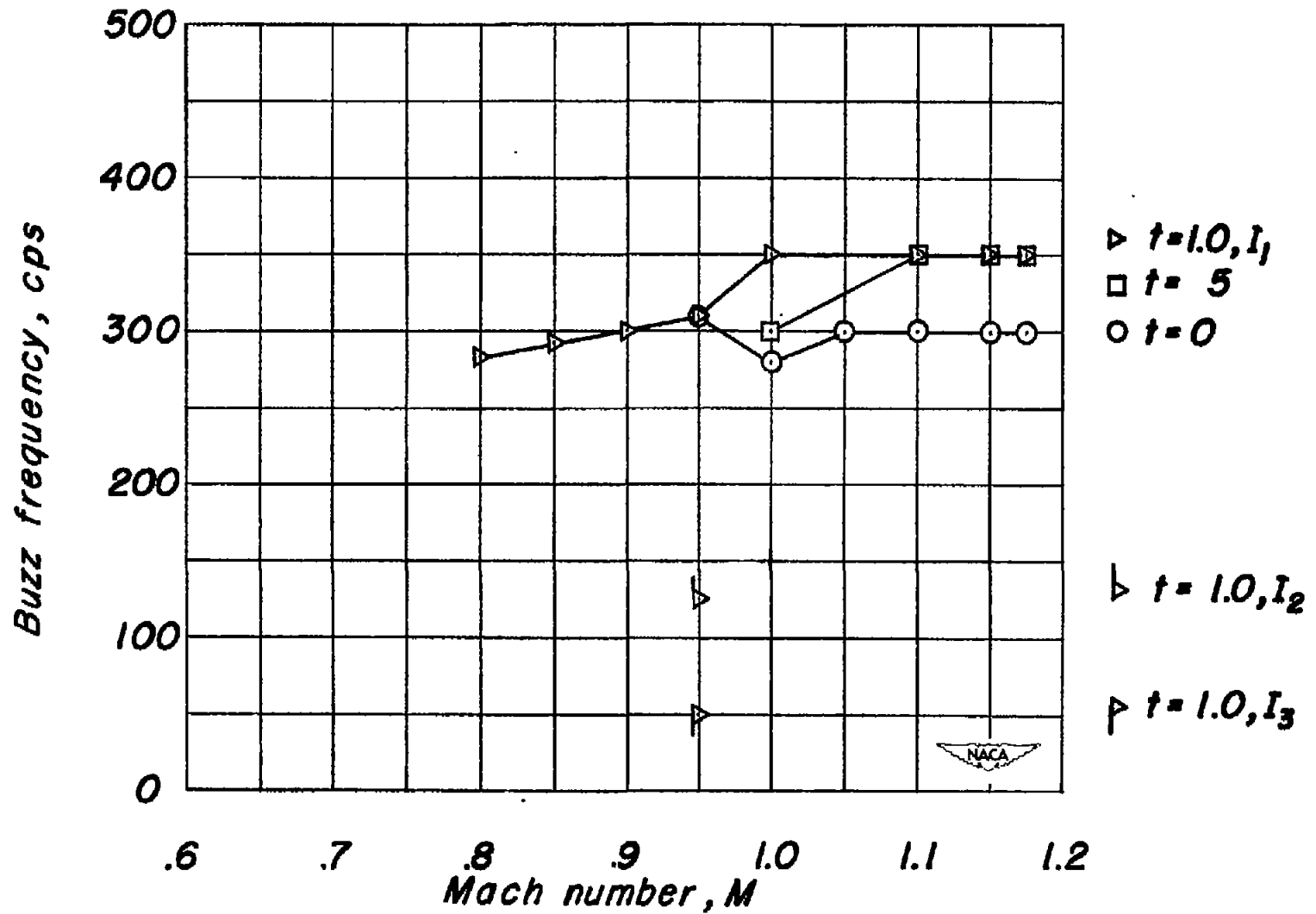


Figure 16.- Effect of Mach number and aileron moment-of-inertia on buzz frequency.

NASA Technical Library



3 1176 01436 2447